2-7-2012

Diversification and expression of the PIN, AUX/LAX, and ABCB families of putative auxin transporters in *Populus*

Nicola Carraro
Purdue University

Tracy Elizabeth Tisdale-Orr
Harvard University

Ronald Matthew Clouse

Anne Sophie Knöller
Philipps University

Rachel Spicer
Connecticut College, rspicer@conncoll.edu

Follow this and additional works at: http://digitalcommons.conncoll.edu/botanyfacpub
Part of the Botany Commons, and the Plant Breeding and Genetics Commons

Diversification and expression of the PIN, AUX/LAX, and ABCB families of putative auxin transporters in *Populus*

Nicola Carraro[1], Tracy Eizabeth Tisdale-Orr[2], Ronald Matthew Clouse[3], Anne Sophie Knöller[4] and Rachel Spicer[5]*

[1] Department of Horticulture and Landscape Architecture, Purdue University, West Lafayette, IN, USA
[2] Rowland Institute at Harvard, Cambridge, MA, USA
[3] Division of Invertebrate Zoology, American Museum of Natural History, New York, NY, USA
[4] Department of Mathematics and Computer Science, Philipps University, Marburg, Germany
[5] Department of Botany, Connecticut College, New London, CT, USA

Intercellular transport of the plant hormone auxin is mediated by three families of membrane-bound protein carriers, with the *PIN* and *ABCB* families coding primarily for efflux proteins and the *AUX/LAX* family coding for influx proteins. In the last decade our understanding of gene and protein function for these transporters in *Arabidopsis* has expanded rapidly but very little is known about their role in woody plant development. Here we present a comprehensive account of all three families in the model woody species *Populus*, including chromosome distribution, protein structure, quantitative gene expression, and evolutionary relationships. The *PIN* and *AUX/LAX* gene families in *Populus* comprise 16 and 8 members respectively and show evidence for the retention of paralogs following a relatively recent whole genome duplication. There is also differential expression across tissues within many gene pairs. The *ABCB* family is previously undescribed in *Populus* and includes 20 members, showing a much deeper evolutionary history, including both tandem and whole genome duplication as well as probable gene loss. A striking number of these transporters are expressed in developing *Populus* stems and we suggest that evolutionary and structural relationships with known auxin transporters in *Arabidopsis* can point toward candidate genes for further study in *Populus*. This is especially important for the ABCBs, which is a large family and includes members in *Arabidopsis* that are able to transport other substrates in addition to auxin. Protein modeling, sequence alignment and expression data all point to ABCB1.1 as a likely auxin transport protein in *Populus*. Given that basipetal auxin flow through the cambial zone shapes the development of woody stems, it is important that we identify the full complement of genes involved in this process. This work should lay the foundation for studies targeting specific proteins for functional characterization and *in situ* localization.

Keywords: auxin, PIN, AUX/LAX, ABCB, *Populus*

INTRODUCTION

Plant development is highly plastic owing to growth via meristems, and this plasticity is fundamental to the ability of plants, as sessile organisms, to adapt to changing environments. Developmental flexibility is particularly important for trees, which can live for thousands of years in the same place, growing massive bodies that must face a multitude of environmental challenges. The plant hormone auxin is well established as a key regulator of plant morphogenesis and in recent years the molecular mechanisms of transport and action have been elucidated. With the publication of the *Populus trichocarpa* genome (Tuskan et al., 2006), new tools to improve our understanding of secondary growth — the type of vascular growth that defines woody plants — became available. *Populus* is not only the dominant model species for woody plant growth, but also a valuable crop for pulp, bioenergy production, and carbon sequestration. Thus, understanding the mechanisms that underlie auxin transport in *Populus* is of interest both in the

context of the evolution of plant development and as a means to manipulate plant architecture, biomass production, and fiber quality.

The auxins as a group include several molecules, with the most abundant natural form in plants being indole-3-acetic acid (IAA). Auxin synthesis occurs in young, actively growing tissues including shoot tips, young leaves, and germinating seeds (Ljung et al., 2001a,b), and increasing evidence suggests that synthesis takes place in the roots as well (Ljung et al., 2005). Auxin moves from the sites of production throughout the plant via two routes: long distance transport of conjugated forms in the phloem and short distance transport of "free" (non-conjugated) auxin via polar auxin transport (PAT). By far the better studied route, PAT is a form of active intercellular transport mediated by proteins inserted in the plasma membrane that belong to three distinct families. The *PIN* and *ABCB* families encode efflux proteins (i.e., proteins that facilitate movement out of cells), whereas members of the

AUX/LAX family facilitate auxin entry into cells, along with passive diffusion. PAT is relatively slow (5–20 mm/h; Lomax et al., 1995), saturable and can be impaired by the application of both competitive inhibitors and inhibitors of protein synthesis (Katekar and Geissler, 1980; Sussman and Goldsmith, 1981). This form of transport is considered polar because the protein carriers are often asymmetrically positioned in the plasma membrane such that transport is directional. Transport directionality can then be altered on relatively short timescales in response to repositioning of the protein carriers. Feedback mechanisms also exist such that PAT is often self-reinforcing, with multiple transport proteins themselves being upregulated by auxin (Sauer et al., 2006; Titapiwatanakun and Murphy, 2009).

The PIN proteins have been studied extensively in *Arabidopsis thaliana* (Chen et al., 1998; Luschnig et al., 1998; Müller et al., 1998; Utsuno et al., 1998; Friml et al., 2002a,b, 2003) and show dynamic polar localization at the plasma membrane (PIN1, PIN2, PIN3, PIN7) or in the endoplasmic reticulum (ER) (PIN5, PIN6, PIN8; Mravec et al., 2009; Friml and Jones, 2010). PIN1 was first described as mediating PAT and determining organ outgrowth at the inflorescence (Okada et al., 1991; Gälweiler et al., 1998; Vernoux et al., 2011). Subsequently its role in embryogenesis, vein patterning, vascular development, and root development were established (Friml et al., 2003; Vieten et al., 2005; Scarpella et al., 2006; Petrásek and Friml, 2009). The characterization of PIN genes has been expanded to include the monocotyledons *Zea mays* and *Oryza sativa*, both of which express several PINs thought to be specific to the monocots. In maize, ZmPIN1a, b, and c are responsible for directing auxin transport in the male and female inflorescences and in the floret meristems (Carraro et al., 2006; Wu and McSteen, 2007). They are also involved in endosperm and embryonic development (Forestan et al., 2010) and in the maintenance of phyllotaxy (Lee et al., 2009). The monocot-specific PINs from rice (OsPIN9, OsPIN10a, and OsPIN10b) are highly expressed in adventitious root primordia and pericycle cells at the stem-base, suggesting that they may have evolved to promote adventitious root development (Wang et al., 2009).

Members of the *AUXIN/LIKE AUXIN* (*AUX/LAX*) family in *Arabidopsis* (Bennett et al., 1996; Yemm et al., 2004) are largely responsible for auxin influx, although the protonated form of auxin (IAAH) is able to passively diffuse into cells. The founder member *AUX1* encodes a plasma membrane protein that belongs to the amino acid permease family of proton-driven transporters and functions as an anionic symporter (Swarup et al., 2005; Yang et al., 2006). AUX1-mediated IAA uptake is implicated in gravitropic response, as the agravitropic phenotype of the *aux1* mutant can be phenocopied in wild-type seedlings by applying the auxin influx carrier inhibitor 1-naphthoxyaceticacids (1-NOA) and rescued using the membrane-permeable auxin 1-naphthaleneacetic acid (NAA; Swarup et al., 2001; Yemm et al., 2004). The paralogs of *AUX1*, *LAX1*, *LAX2*, and *LAX3* encode proteins that maintain a correct phyllotactic pattern at the shoot apical meristem (SAM), as they act together with PIN1-mediated auxin efflux (Bainbridge et al., 2008). *LAX3* is also involved in the development of lateral root primordia (Swarup et al., 2008).

The involvement of ABCB [ATP-binding cassette (ABC) transporters of the B class, previously known as multidrug resistance (MDR)/Phosphoglycoprotein (PGP)] proteins in auxin transport was first hypothesized when expression of ABCB1/PGP1 in *Arabidopsis* was found to regulate hypocotyl elongation in a light-dependent fashion (Sidler et al., 1998). Subsequently, ABCB1 was shown to function with ABCB19/PGP19/MDR1 in mediating PAT (Noh et al., 2001). ABCB1 and ABCB19 are the closest *Arabidopsis* orthologs of mammalian ABCB1-type MDR transporters and although specificity for auxin is not assured (Lee et al., 2008), some appear to transport auxin with relatively high substrate specificity (Titapiwatanakun and Murphy, 2009; Yang and Murphy, 2009). ABCB14 and ABCB15 promote auxin transport along the inflorescence of *Arabidopsis*, where they are expressed in vascular tissue and interfascicular fibers. Inflorescence stems in both knockout mutants show a reduction in PAT (Kaneda et al., 2011). ABCB4 from *Arabidopsis* is involved in basipetal PAT in the root (Terasaka et al., 2005; Wu et al., 2007; Kubeš et al., 2011) and, although most ABCBs studied to date function as efflux carriers, heterologous expression of ABCB4 suggests that it functions as an auxin influx carrier under low concentrations of IAA and reverses to efflux when IAA concentrations increase (Yang and Murphy, 2009). The *ABCB1/PGP1* ortholog has been cloned in maize (*Brachytic2/ZmPGP1*) and in *Sorghum bicolor* (*dwarf3/SbPGP1*) and shown to be responsible for IAA transport along the stem (Multani et al., 2003; Knöller et al., 2010).

Our understanding of PAT and its role in development has advanced considerably in *Arabidopsis* and to a lesser extent in monocots, but the functional significance of these transport proteins — particularly the ABCBs — remain largely unknown in woody plants. Woody plants are defined by the production of secondary vascular tissue, specifically secondary xylem and phloem. These vascular tissues are derived from a lateral meristem called the vascular cambium that encircles the stem, adding new cells that will ultimately differentiate into xylem toward the inside of the stem and phloem toward the outside. Given the demonstrated role of PAT in vascular development in herbaceous plants it seems logical to expect a role in secondary growth. Indeed, the vascular cambium contains high levels of IAA in both *Pinus* and *Populus*, with a peak concentration occurring either in the cambial initials themselves, or perhaps more likely, in the earliest differentiating xylem elements (Uggla et al., 1996, 1998; Tuominen et al., 1997; Hellgren et al., 2004). Concentrations rapidly decline through the regions of cell differentiation to near zero in mature secondary xylem and phloem. Auxin transport in the cambium is basipetal (Lachaud and Bonnemain, 1984; Uggla et al., 1998; Kramer et al., 2008) and several members of the *PIN* and *AUX/LAX* gene families are expressed in developing *Populus* stems (Schrader et al., 2003, 2004; Nilsson et al., 2008). Furthermore, expression of one or more *PIN* and *AUX/LAX* genes is downregulated with the onset of dormancy (Schrader et al., 2003, 2004) and upregulated following exogenous application of IAA and/or gibberellins (Schrader et al., 2003; Björklund et al., 2007). Despite several excellent studies in *Populus*, our knowledge of the molecular mechanisms that regulate PAT in woody plants is essentially restricted to the expression patterns of just three *PIN* and *AUX/LAX* genes. A more comprehensive understanding of PAT gene and protein function in *Populus* will help to clarify the molecular mechanisms controlling vascular pattering in woody plants and explain the link(s) between

short and long distance auxin transport in species with extensive stem development.

Here we present the first comprehensive account of the *PIN*, *AUX/LAX*, and *ABCB* gene families in *Populus*, which contain 16, 8, and 20 members respectively. We investigate the history of gene family members relative to each other within *Populus* and relative to proposed orthologs in *Arabidopsis*. Through phylogenetic analysis we describe the timing of the diversification of the *PIN*, *AUX/LAX*, and *ABCB* gene families relative to when plants colonized land. Because the transport function of the ABCB proteins is less understood and their specificity for auxin has not been completely elucidated, we model the protein structures for *Populus* ABCBs and compare these to known *Arabidopsis* ABCB transporters. We then provide expression data for all putative auxin transporters in *Populus*, including presence or absence data for each gene in the cortex, phloem, cambial zone, and xylem of mature stems. We present quantitative RT-PCR expression levels for whole plantlets, internodes just beginning to form secondary vascular tissue, roots and developing xylem from mature stems. Lastly, in order to determine the most likely contributors to the positive feedback mechanism driving "canalization" of auxin flow during vascular development, we test the response of *PIN*, *ABCB*, and *AUX/LAX* genes to exogenous IAA application. These findings should lay the foundation for the functional characterization of members of each family and suggest which proteins are likely to be important regulators of secondary growth.

MATERIALS AND METHODS
PLANT MATERIAL
Populus tremula × alba hybrid clone INRA 717-1B4 was chosen for all experimental procedures. *In vitro* plants were grown on half-strength Murashige and Skoog (MS) supplemented with 2% sucrose, 0.25 mg ml^{-1} MES, 0.04 mg ml^{-1} glycine, and 0.2 mg ml^{-1} myo-inositol at $25 \pm 2°$C under 16 h day length conditions using GE 20W F20T12 growth lamps. Greenhouse plants were grown in 2:1:1 promix HP: perlite:vermiculite supplemented with 19–6–12 N–P–K slow release fertilizer. Greenhouse temperatures were maintained around $22 \pm 5°$C and day light supplemented to achieve a 16 h day length using metal halide lamps.

IDENTIFICATION OF *PIN*, *AUX/LAX*, AND *ABCB* GENE AND PROTEIN FAMILIES
Populus trichocarpa gene and protein sequences were retrieved from the Joint Genome Institute's (JGI) *P. trichocarpa* v.1.1 database[1]. Henceforth we refer to these genes and gene families as *PtrPIN*, *PtrAUX*, and *PtrABCB*. When reporting expression data, we will refer to the same genes from *P. tremula × alba* (abbreviated as *Pta*, i.e., *PtaPIN1*). The *PIN* and *AUX/LAX* sequences had been previously annotated and we maintained the original nomenclature including the *AUX* and *LAX* names for every member of the *AUX/LAX* family from *P. trichocarpa* (i.e., *PtrAUX1–LAX5*). Every sequence was used as query with the BLASTn algorithm to search the National Centre for Biotechnology Information (NCBI)

nucleotide collection database to confirm sequence identity. Putative *ABCB* genes in the *P. trichocarpa* genome were identified in the same database using 22 *Arabidopsis ABCB* gene sequences retrieved from the *Arabidopsis* Genome Initiative Research database (TAIR)[2]. The JGI *P. trichocarpa* v.1.1 database was also searched using the terms "MDR" and "ATP" as queries. A third search was conducted using the retrieved sequences to interrogate the *Populus* DataBase (PopulusDB)[3]. Finally all retrieved sequences were confirmed as encoding putative auxin transporters by searching the phytozome v.7.0 database[4]. All the remaining *PIN*, *AUX/LAX* and *ABCB* sequences from other species were retrieved from phytozome v.7.0, TAIR10, The Rice Genome Annotation Project[5], and MaizeGDB[6]. The complete list of retrieved genes is provided in **Table A4** in Appendix. All sequences were inspected for redundancy and presence of pseudogenes and invalid gene models were discarded. ABCB protein sequences were used as queries to search the PROSITE database[7] to confirm the presence of the TMD–NBD–TMD–NBD (transmembrane domain, nucleotide-binding domain) structure and the ABC C-motif. This allowed to rule out the presence of ABC half transporters and other ABC proteins not belonging to class B (Sanchez-Fernandez et al., 2001) and to classify the genes according to their full length structure, conserved motifs, sequence similarity, and EST support. Intron–exon structures of *P. trichocarpa PIN*, *AUX/LAX*, and *ABCB* genes were produced using the online tool GSDS, Gene Structure Display Server (Guo et al., 2007)[8]. The genome representation for *Populus* was created using the online tool SyMAP v.3.5[9]

PtrABCB, PIN, AND AUX/LAX STRUCTURE ANALYSIS AND PtrABCB MODELING
Transmembrane domains were predicted using the online tools TMHMM Server v.2.0[10] and Aramemnon[11]. The protein structure of Sav1866 and MDR1 were obtained from the PDB (Protein Data Bank) database[12]. The predicted protein structures of AtABCB1 and 4 have been previously generated by Yang and Murphy (2009). *Arabidopsis* templates (ABCB1 or 4) were chosen based on closest sequence identity. To generate the alignment files of *Populus* ABCB protein sequences and *Arabidopsis* ABCB sequences, Multialin[13] was used with default settings. The output file was manually edited to meet Modeller 9v5 requirements[14]. The predicted 3D protein structure was generated using the python script Modeller 9v5. Three structures were generated and the quality was determined according to the manual (Wiederstein and Sippl, 2007). The best model was used for substrate docking. Furthermore, the

---

[1] http://genome.jgi-psf.org/Poptr1_1/Poptr1_1.home.html

[2] www.arabidopsis.org
[3] http://www.populus.db.umu.se
[4] http://www.phytozome.org
[5] http://rice.plantbiology.msu.edu/
[6] http://www.maizegdb.org/
[7] http://ca.expasy.org/prosite/
[8] http://gsds.cbi.pku.edu.cn/index.php
[9] http://www.symapdb.org/.
[10] http://www.cbs.dtu.dk/services/TMHMM/
[11] http://aramemnon.uni-koeln.de/
[12] http://www.rcsb.org/pdb/home/home.do
[13] http://bioinfo.genotoul.fr/multalin/multalin.html
[14] http://salilab.org/modeller/release.html

quality of the protein model was tested using the program ProSA[15]. Substrate docking was performed using MEDOCK[16]. PDB files of all proteins were translated into pdbq files using the PDB2PQR server[17]. For substrate docking prediction, the nucleotide-binding folds (NBFs) were removed. All loops connecting the TMDs were removed to reduce the size of the file. Finally, the pdbq file of IAA was produced with the Dundee PRODRG2 Server (Dolinsky et al., 2004, 2007)[18]. Each run had a docking repeat of five times and four runs were performed, resulting in a total of 20 molecules docked to the protein structure. Protein models were displayed using PyMol[19].

PHYLOGENETIC ANALYSIS

Phylogenic reconstruction was conducted using the coding sequences of 18 species, including 3 monocotyledonous and 10 dicotyledonous plants. Sequences from the green algae *Chlamydomonas reinhardtii* (Merchant et al., 2007) and *Volvox carteri* (Prochnik et al., 2010), the moss *Physcomitrella patens* (Rensing et al., 2008) and the lycopod *Selaginella moellendorffii* (Banks et al., 2011) were also included. For each coding sequence, three types of trees were retrieved from two different alignments. The first alignment was generated in concert with the tree search, a method called "dynamic homology" (Wheeler, 1996). 149, 68, and 245 unaligned coding sequences from the *PIN*, *AUX/LAX*, and *ABCB* families (**Table A4** in Appendix) were read into the phylogenetic program POY v.4.1.2 (Varón et al., 2009) and trees and alignments were searched simultaneously for the least costly sequence alignment and tree topology combination under the parsimony criterion. A second alignment was generated in the program MAFFT (Katoh et al., 2009), where the same sequences were aligned under a gap opening cost of 4 and a gap extension cost of 0.05. This alignment was then input to the program Gblocks v.0.91b (Castresana, 2000; Talavera and Castresana, 2007), which removes regions with multiple gaps and of dubious homology. Gblocks was run with default settings, except that gaps were allowed in all parts of the resulting alignment (such as in cases where one or a few sequences have a clear insertion or deletion). The alignment output by Gblocks was then used for tree searching in POY, where it was read as pre-aligned. Both unaligned and aligned POY tree searches were immediately followed by bootstrap searches, where 100 pseudoreplicates were searched starting with one Wagner tree each. Tree searches were conducted on a parallel computing cluster, using 24 processors searching for a maximum of 6 h of automated searching (in which POY decides on the best combination of builds, swapping, ratchet, and fusing) with dynamic homology and 16 processors for the pre-aligned data. For dynamic homology, in both the tree searches and the bootstrap calculations, the data were divided by the program into seemingly homologous blocks before searching using the command "auto_sequence_partition," which greatly increases search speed. For all POY searches, the costs of

transitions, transversions, and insertion/deletion events were the same.

The alignment from Gblocks was also used for a maximum likelihood search in RaxML (Stamatakis et al., 2008) on the CIPRES Science Gateway (Miller et al., 2010)[20]. The alignment was first uploaded and converted to relaxed Phylip format and then tree searches were performed with likelihood bootstrap in which the best tree is reported along with the results of a 100-pseudoreplicate bootstrap calculation. The program was allowed to determine the best model (the GAMMA Model was chosen) and other parameters automatically before tree searching. All trees were visualized and edited using FigTree v.1.3.1[21]

DNA AND RNA ISOLATION AND cDNA SYNTHESIS

Total RNA from whole *in vitro*-grown plantlets, internodes, roots, and developing xylem was extracted using the Spectrum Plant Total RNA Kit (Sigma-Aldrich, St. Louis, MO, USA) according to manufacturer's instructions. Aliquots of approximately 100 mg developing xylem tissue were homogenized with a Mini Bead Beater (BioSpec Products Inc., Bartlesville, OK, USA) and stainless steel beads. mRNA from 20 μm-thick frozen sections from the cortex, secondary phloem, cambium, and secondary xylem was extracted using the DynaBeads mRNA Direct Kit (Invitrogen, Carlsbad, CA, USA) according to manufacturer's instructions. DNA was extracted using the DNeasy Plant Mini Kit (Qiagen, Valencia, CA, USA) according to manufacturer's instructions using approximately 100 mg fresh leaf tissue. DNA and RNA concentrations were measured with a NanoDrop 2000™ (Thermo Scientific, Waltham, MA, USA). Total RNA was treated with TURBO DNA-free™ (Ambion, Austin, TX, USA) according to manufacturer's instructions. cDNA was synthesized from 1.5 μg of total RNA using SuperscriptII reverse transcriptase (Invitrogen, Carlsbad, CA, USA) with the oligodt$_{20}$ primer. RT-PCR reaction cycles were carried out according to manufacturer's instructions including a final 20 min incubation step with RNAseH (Invitrogen, Carlsbad, CA, USA). cDNA concentration was measured with a Nanodrop 2000™ and the cDNA was diluted to 170 ng μl^{-1}.

AMPLIFICATION, CLONING AND SEQUENCING OF 3′ END PCR PRODUCTS

In order to amplify the 3′ end untranslated region (UTR) of transcripts that could not be detected in quantitative real time PCR (qRT-PCR) reactions with at least three different primer pairs, reverse transcription reactions were carried out using the Adp1-dt17 primer (Kramer et al., 1998) and SuperscriptII reverse transcriptase according to manufacturer's instructions. cDNA was amplified using the Adp1 primer coupled to the corresponding forward primer specifically designed to amplify the 3′ end of the transcript (the complete list of primers is provided in **Table A5** in Appendix). The PCR amplifications were carried out with Taq DNA polymerase (SIGMA, St. Louis, MO, USA) or Amplitaq® Gold DNA polymerase (Applied Biosystems™, Foster City, CA, USA) according to manufacturer's instructions. PCR

---

[15] http://www.came.sbg.ac.at/typo3/index.php?id=prosa

[16] http://medock.csbb.ntu.edu.tw

[17] http://pdb2pqr.sourceforge.net

[18] http://davapc1.bioch.dundee.ac.uk/prodrg,

[19] http://pymol.sourceforge.net

[20] http://www.phylo.org/news/raxml.php

[21] http://tree.bio.ed.ac.uk/software/figtree/.

products were run on 1% agarose gels, gel purified using the Zymo-clean™Gel DNA Recovery Kit (Zymo Research, Irvine, CA, USA) and cloned into the *pGEM*®-T Easy Vector Systems (Promega, Madison, WI, USA). Colonies were grown on LB plates containing 100 mg/ml ampicillin. Following PCR amplification, positive colonies were grown in 4 ml of LB medium containing 100 mg/ml ampicillin, at 37°C, over night. Plasmid DNA was extracted using the Qiagen Plasmid Mini Kit (Qiagen, Valencia, CA, USA) according to manufacturer's instructions. Plasmids were sequenced by Eurofins MWG Operon (Huntsville, AL, USA). Sequences were aligned using the Vector NTI Advance™10.3.0 AlignX module (Invitrogen, Carlsbad, CA, USA).

QUANTITATIVE RT-PCR

Quantitative real time PCR was carried out on the MX3000P and MX3005P systems (Stratagene, La Jolla, CA, USA) using Brilliant™SYBR® Green QPCR Master Mix (Stratagene, La Jolla, CA, USA) according to manufacturer's instructions. The SYBR® Green (with dissociation curve) experimental setup was used. Plates were manually loaded and reactions were carried out in a total volume of 20 μl, using 75 ng of cDNA per reaction. Reactions were run in triplicate. Primer pairs were designed using Primer3 software[22], analyzed with OlygoAnalyzer 3.1 software[23] for melting temperature, oligo-, hetero-dimer, and hairpin structure formation, synthesized by Integrated DNA Technologies (IDT, IA) and tested with conventional PCR to verify amplification of a single product. Following primer titration, a final concentration of 250 nM for each primer was chosen. In qRT-PCR experiments the following thermal cycling conditions were used: activation step of 10 min at 95°C; 40 cycles of 30 s at 95°C, 25 s at 57°C, 25 s at 72°C; fluorescence was collected at the end of each extension step. A melting curve analysis was performed.

Efficiency-corrected expression values were calculated based on standard curves for all genes (Livak and Schmittgen, 2001; Pfaffl, 2001). Standard curves were run in triplicate for every gene in every cDNA batch and amplification efficiencies were calculated from the standard curve slopes. Baseline-subtracted and ROX-normalized fluorescence readings were collected with the MX3005P software v.4.01. Expression values were normalized to the geometric mean of four housekeeping genes (*PtaPD-E1*, *PtaUBQ1*, *PtaTUA2*, *PtaACT2*) that were found, in our hands, to have the highest amplification efficiency and most stable expression across different tissues (Vandesompele et al., 2002; Brunner et al., 2004; Gutierrez et al., 2008). For expression following exogenous IAA application, the same set of normalizers was used in a comparative quantitation experiment comparing treated and untreated control tissues.

IAA TREATMENTS

Two-month-old *P. tremula × alba* was grown in the greenhouse. Approximately 1-cm-long segments of internodes between four and eight nodes beneath the shoot apex and actively growing root tips were collected and incubated at room temperature in 30 μM IAA in liquid growth media (half-strength MS salts, 2% sucrose,

0.25 mg ml⁻¹ MES, 0.04 mg/ml glycine, and 0.2 mg ml⁻¹ myo-inositol) for 6 h in the dark following a 15 min vacuum infiltration. The same conditions were used for negative controls (no IAA). Tissues were frozen in liquid N_2 and ground for RNA extraction.

RESULTS

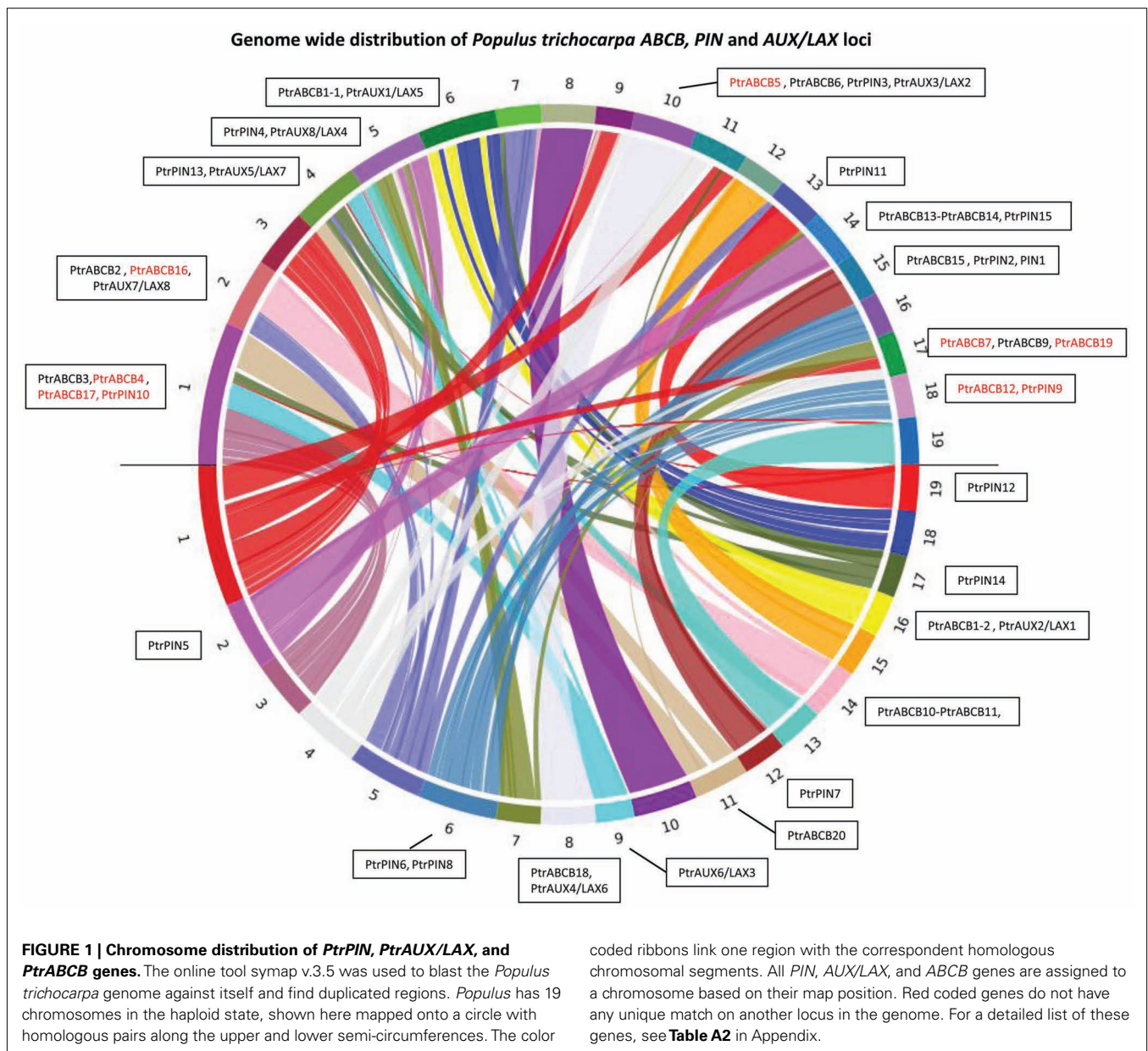### CHROMOSOMAL DISTRIBUTION AND GENE DUPLICATION IN THE *PIN, AUX/LAX,* AND *ABCB* FAMILIES OF *POPULUS*

Nearly every locus coding for a PIN, AUX/LAX, or ABCB protein has a corresponding paralogous locus in another chromosomal block (**Figure 1**). *Populus* has exactly twice the number of *PIN* (16) and *AUX/LAX* (8) genes as *Arabidopsis* (eight and four, respectively) and these genes form pairs with highly similar coding sequences, which may be the consequence of the relatively recent genome duplication (**Figures 1, 2,** and **3**). Neither the *PIN* loci nor the *AUX/LAX* loci appear to be derived from tandem duplications. In contrast, three tandem duplicated *ABCB* loci pairs (*PtrABCB2–PtrABCB8*, *PtrABCB10–PtrABCB11*, and *PtrABCB13–PtrABCB14*) are present in the *Populus* genome. Unlike the *PIN* and *AUX/LAX* families, the *ABCB* genes are more randomly distributed between corresponding and non-corresponding duplicated regions, with nine members that do not present any paired gene on another chromosome (**Figure 1**).

GENE AND PROTEIN STRUCTURE OF THE *PIN, AUX/LAX,* AND *ABCB* FAMILIES OF *POPULUS*

We identified a total of 44 *Populus* genes encoding putative auxin transport proteins, including 16 *PIN*, 8 *AUX/LAX*, and 20 *PtrA-BCB* loci. The complete list of *P. trichocarpa PIN, AUX/LAX,* and *ABCB* gene names, gene models, and loci can be found in **Table A2** in Appendix. The PIN genes of *Populus* present a conserved intron–exon organization which is illustrated in **Figure A1** in Appendix. The same structural characteristics are present across PINs from different plant species including *Arabidopsis* (Mravec et al., 2009; Wang et al., 2009; Shen et al., 2010). The proteins belonging to the PtrPIN family range from 347 to 650 amino acids in length. In *Populus*, seven, three, and six PIN proteins present long, reduced and short central hydrophilic domains respectively. In general, there is no strict correlation between the length of the genomic sequence of loci coding for auxin transporters and their protein product length (**Figure A1** and **Table A3** in Appendix). One locus (*PtrPIN14*) is classified as encoding a pseudogene. The proteins for the PtrAUX/LAX family range from 465 to 492 amino acids and present the most conserved sequence among the three families of putative auxin transporters. Their primary sequence is generally conserved across the plant kingdom and *Populus* has twice the number of *AUX/LAX* coding loci compared to *Arabidopsis*. All of the PtrAUX/LAX proteins have 11 predicted transmembrane domains. All the *ABCB* loci from *P. trichocarpa* encode proteins with a repeated TMD–NBD structure and carry a predicted nucleotide-binding domain signature ([AG]- × (4)-G-K-[ST]; Rea, 2007; Verrier et al., 2008). Their length varies between 1141 and 1578 amino acids and the two regions integral to the plasma membrane are highly hydrophobic and comprise 7–12 transmembrane helices. In addition to these two conserved modules, a more variable and less hydrophobic linker region connects the first NBD to the second TMD in all PtrABCB proteins.

---

[22] http://frodo.wi.mit.edu/primer3
[23] http://www.idtdna.com/analyzer/Applications/OligoAnalyzer

FIGURE 1 | Chromosome distribution of *PtrPIN, PtrAUX/LAX,* and *PtrABCB* genes. The online tool symap v.3.5 was used to blast the *Populus trichocarpa* genome against itself and find duplicated regions. *Populus* has 19 chromosomes in the haploid state, shown here mapped onto a circle with homologous pairs along the upper and lower semi-circumferences. The color coded ribbons link one region with the correspondent homologous chromosomal segments. All *PIN, AUX/LAX,* and *ABCB* genes are assigned to a chromosome based on their map position. Red coded genes do not have any unique match on another locus in the genome. For a detailed list of these genes, see **Table A2** in Appendix.

IDENTIFICATION OF PREDICTED IAA MEMBRANE TRANSPORTERS FROM THE ABCB FAMILY OF *POPULUS*

After analysis of the primary structure of the PtrABCB proteins, models of tertiary structure were produced using all 20 ABCB amino acid sequences. Structural models were displayed using PyMol (**Figure A2** in Appendix) in order to determine which PtrABCBs are the most likely candidates for IAA transport. Although pairwise comparison of amino acid sequences can provide a first estimate of which proteins are the true orthologs of confirmed *Arabidopsis* auxin transporters (AtABCB1, AtABCB19, and AtABCB4), this information should be supported with the identification of IAA docking sites and transmembrane barrel structure predictions (Yang and Murphy, 2009). Among all PtrA-BCBs, 10 are predicted to have one or more IAA binding sites (**Figure A2** in Appendix). In *Arabidopsis*, IAA is primarily docked

at two binding sites in the TMDs of ABCB19 while ABCB4 has a unique additional binding site (Yang and Murphy, 2009). In *Populus*, ABCB1.1/ABCB1.2 and ABCB19 have the most similar sequence to AtABCB1 and AtABCB19 and have two, five, and three predicted binding pockets respectively.

RECONSTRUCTION OF THE PHYLOGENETIC RELATIONSHIPS IN THE *PIN*, *AUX/LAX*, AND *ABCB* GENE FAMILIES OF *POPULUS*

All three phylogenetic analyses (parsimony using unaligned and aligned sequences and maximum likelihood with aligned sequences) generally resulted in well resolved, reasonable, highly supported trees, indicating considerable phylogenetic signal in the sequence data, which was robust to different methods of analysis. Here we show the trees for all three gene families found under maximum likelihood and the tree found under dynamic homology

FIGURE 2 | Phylogeny of the *PIN* genes. Maximum likelihood phylogeny of *PIN* genes from land plants, based upon coding sequences from the loci listed in **Table A4** in Appendix. Gray branches indicate nodes with bootstrap support lower than 50%. Basal land plant *PINs* are colored blue, *Populus* green, *Arabidopsis* red, and monocots yellow. Abbreviated names of each species are listed in **Table A1** in Appendix.

and parsimony for the ABCB family (**Figures 2**, **3**, and **4**; **Figure A3** in Appendix). The three different analyses showed the same general patterns in each gene family, although the *PIN* analysis was more sensitive to the difference between likelihood and parsimony, the latter producing long, pectinate clades containing a mixture of taxonomic groups.

The *PIN* genes of basal land plants (*Physcomitrella* and *Selaginella* in our analysis) cluster at the base of the tree, with the exception of *PpPIN1D* (**Figure 2A**). The placement

of *PpPIN1D* may indicate an erroneous or highly derived sequence, as its placement was unstable and with low bootstrap support and it was recovered in the likelihood tree on an extremely long branch. The angiosperm *PINs* initially split into two large clades, with subsequent splits that show the monocot/dicot divergence four or five times, although support for several of these nodes is weak (**Figure 2**). There is also the frequent occurrence of clear sister pairs of *PINs* in *Populus*.

FIGURE 3 | Phylogeny of the *AUX/LAX* genes. Maximum likelihood phylogeny of *AUX/LAX* genes from land plants, based upon coding sequences from the loci listed in **Table A4** in Appendix. Gray branches indicate nodes with bootstrap support lower than 50%. Basal land plant *AUX/LAX* genes are colored blue, *Populus* green, *Arabidopsis* red, and monocots yellow. Abbreviated names of each species are listed in **Table A1** in Appendix.

The *AUX/LAX* analysis similarly places the basal land plant *AUX/LAX* genes in a grade at the base of the tree followed by two large clades of angiosperms (albeit with weak support; **Figure 3**). The monocot *AUX/LAX* genes were recovered as two closely related clades under maximum likelihood (**Figure 3B**) but were recovered as a single clade when the aligned data were analyzed under parsimony (trees not shown). All *Populus AUX/LAX* genes were recovered as sister pairs or, in the case of *PtrAUX1–LAX5* and *PtrAUX2–LAX1*, as closely related in a clade with the *P. tomentosa* and *P. tremula × tremuloides AUX/LAXs*.
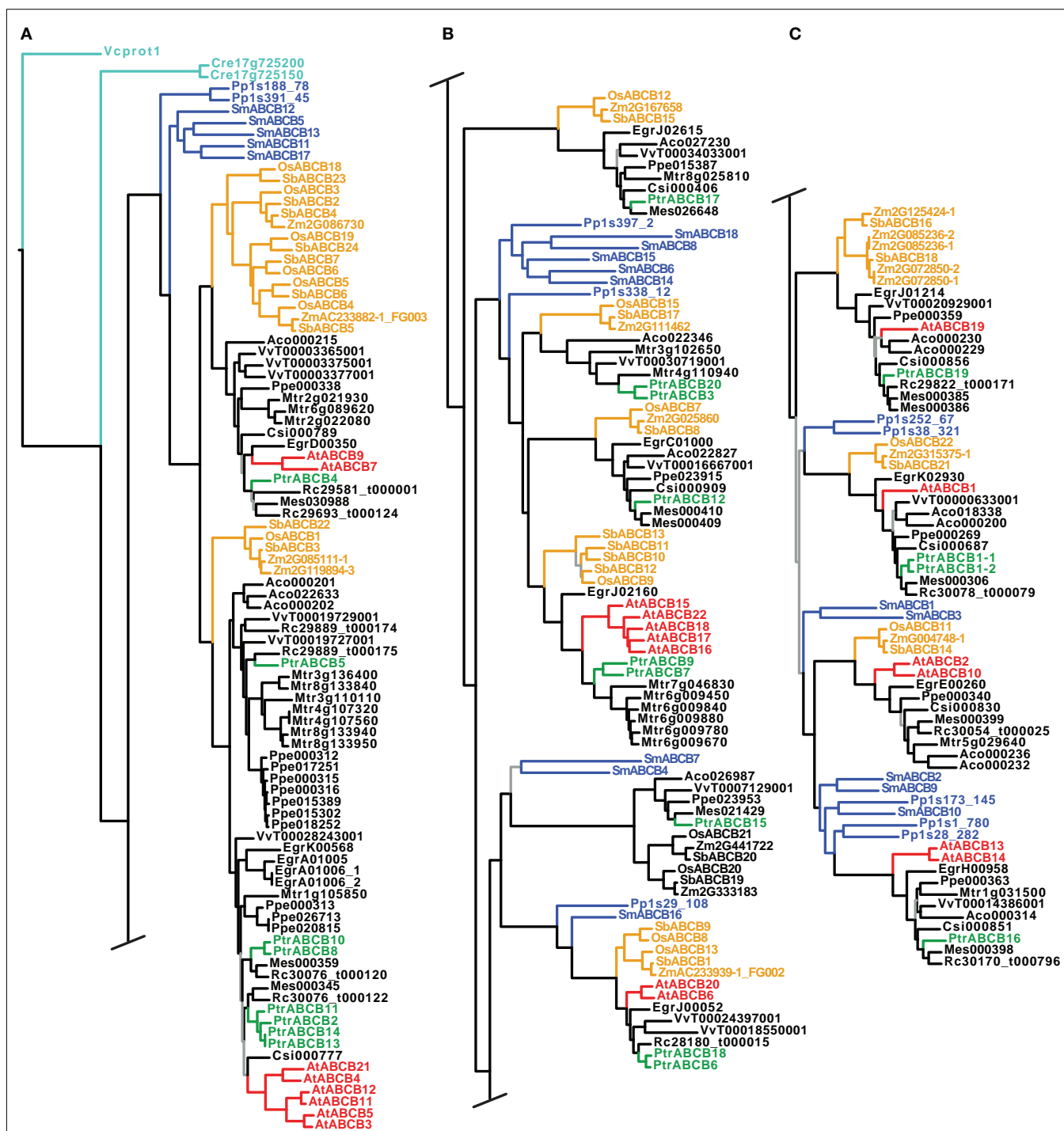
FIGURE 4 | Phylogeny of the *ABCB* genes. Maximum likelihood phylogeny of *ABCB* genes from land plants, based upon coding sequences from the loci listed in **Table A4** in Appendix. Gray branches indicate nodes with bootstrap support lower than 50%. Algal *ABCBs* are colored light blue–green, basal land plants blue, *Populus* green, *Arabidopsis* red, and monocots yellow. Abbreviated names of each species are listed in **Table A1** in Appendix. An alternative phylogeny for the *ABCBs* based on dynamic homology and parsimony, generated with the program POY v.4.1.2, is shown in **Figure A3** in Appendix.

In contrast to the *PIN* and *AUX/LAX* trees, clades, or paraphyletic grades of basal land plant *ABCBs* were recovered in several different locations throughout each tree, often as sister to angiosperm clades that subsequently showed the monocot/dicot split (**Figure 4**). We included coding sequences from the green algae in our *ABCB* analysis: two putative *ABCB* transporters

from *C. reinhardtii* (Cre17_g725200 and Cre17_g725150) and one *ABCB*-like sequence from *V. carteri* (Vcprot1), the latter used to root each *ABCB* tree. The inclusion of the algal sequences and the use of *Volvox* as a root appear valid, as they are not recovered on especially long branches, and *Physcomitrella* and *Selaginella* are appropriately placed on the first branches of each tree. In the maximum likelihood tree, we recovered 10 separate clades of monocot *ABCB*s, as well as an apparent expansion of the *ABCB*s in several angiosperm species, including *Medicago truncatula* and *Prunus persica* (**Figures 4A,B**). Among the *Populus ABCB*s, only few were recovered in clear sister pairs. The tree found under dynamic homology for the *ABCB*s recovered almost identical groupings of basal land plant, monocot, and dicot *ABCB*s as those trees found using aligned sequences, but the relationships among these clades or groups differed. For example, a clade containing *OsABCB12* and *Mes026648* (top of **Figure 4B**) was recovered as a paraphyletic grade immediately after the algal sequences in the dynamic homology tree (**Figure A3A** in Appendix).
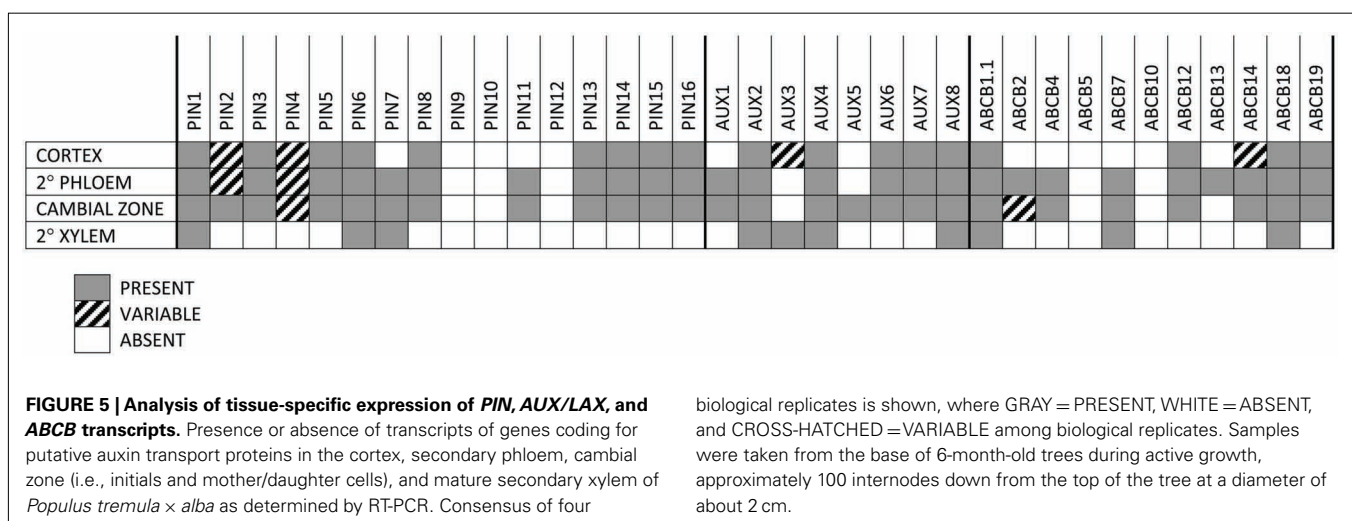
TISSUE-SPECIFIC AND IAA-INDUCED EXPRESSION OF *PtaPINs*, *PtaAUX/LAXs,* AND *PtaABCBs*
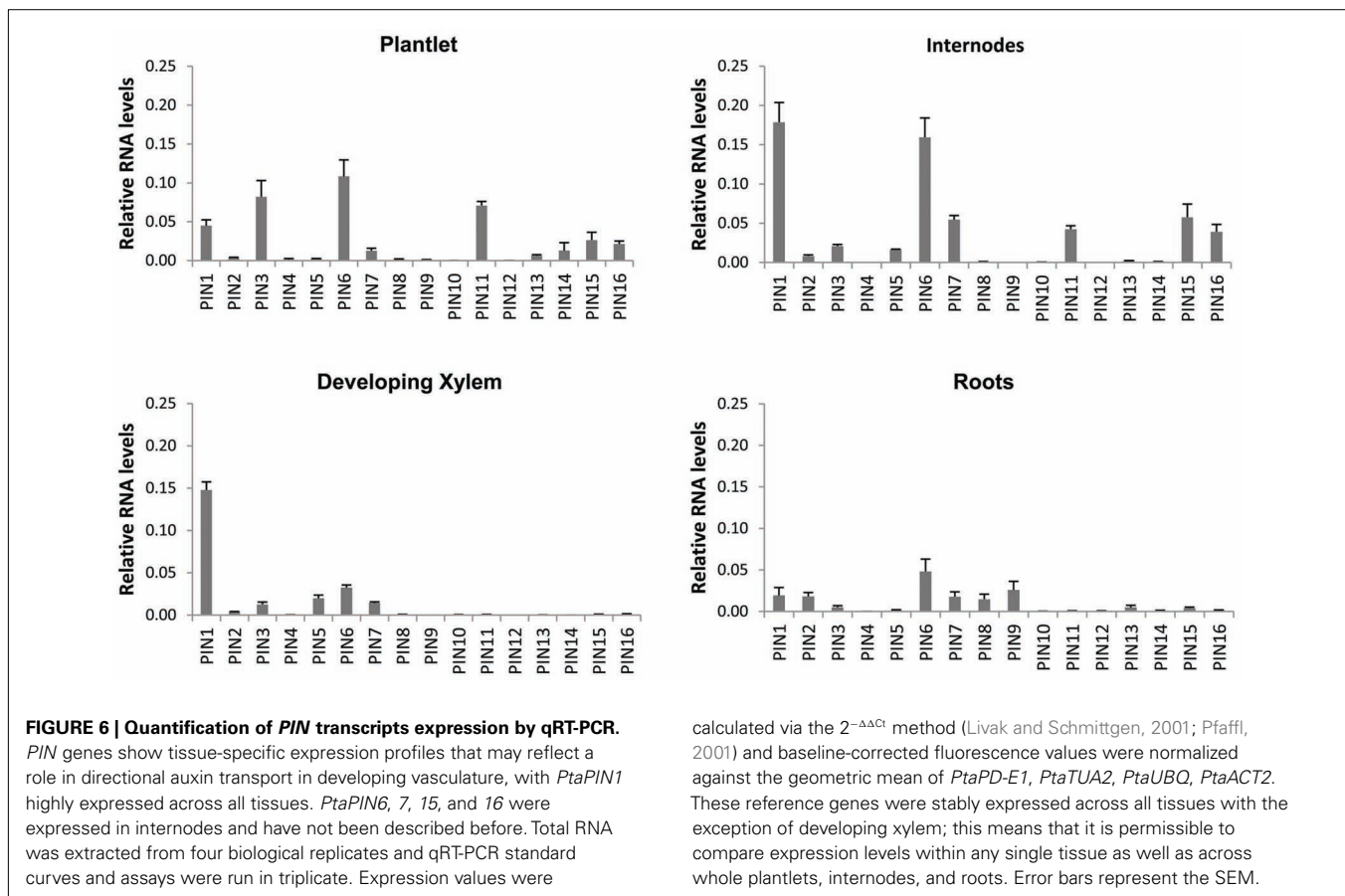
Expression of all *PIN*, *AUX/LAX*, and *ABCB* gene family members in *P. tremula × alba* was characterized for whole plantlets, roots, and stem tissues from several developmental stages through qRT-PCR (**Figures 6–8**). Whole *in vitro*-grown plantlets that were old enough to have initiated secondary growth were used as an initial screen and showed that over half of the *PtaPINs* and *PtaAUX/LAX* genes were expressed at above-trace levels, while only four or five *PtaABCBs* showed above-trace expression. Internodes that spanned the region of secondary growth initiation in greenhouse-grown plants should reflect combined expression in several distinct tissues, including cortex, vascular cambium, developing secondary vasculature, and primary xylem parenchyma. Here *PtaPIN1*, *6*, and *PtaABCB1.1* show high expression levels, with lower levels of *PtaPIN7*, *11*, *15*, *16*, and *PtaABCB7* (**Figures 6** and **8**). Developing secondary xylem removed from beneath the bark in 6-month-old

greenhouse-grown trees showed high expression of *PtaPIN1* and *PtaABCB1.1*, with lower levels of *PtaABCB7*. Roots showed low expression levels of most genes, which may simply reflect the fact that the roots collected were relatively mature and composed largely of parenchyma, rather than a concentration of actively growing root tips. *PtaAUX/LAX* genes were expressed at relatively uniform levels across all tissues and developmental stages (**Figure 7**), although expression levels were highest for developing xylem, where very high levels of *PtaAUX2* were detected.

In order to perform an expression screen (RT-PCR) with higher spatial resolution in developing woody stems, basal internodes approximately 100 nodes and 2.5 m down from the stem apex of 6-month-old *Populus* were freeze-sectioned and tissue collected from the cortex, secondary phloem, cambial zone (restricted to cambial initials and mother/daughter cells), and secondary xylem. Developing secondary xylem and phloem were discarded in order to obtain the most pure collections of tissues possible. Given that, the number of members of all families that are expressed in each tissue is striking (**Figures 5–8**). Only *PtaPIN9*, *10*, and *12* and *PtaABCB5* and *10* were not expressed in any tissue (**Figures 6** and **8**), and although some of the transcripts detected through RT-PCR are likely expressed at very low levels, it is clear that expression of many previously undescribed members (e.g., *PtaPIN6*, *7*, *15*, and *16* and *PtaABCB1.1* and *7*) is widespread in *Populus* stems. Also striking is the fact that several members of all three transport families are expressed in mature secondary xylem, from which all mRNA is derived from living ray parenchyma cells.

Because a positive feedback mechanism is fundamental to the canalization of auxin flow during vascular development, we also tested the auxin response of members of the *PtaPIN*, *PtaAUX/LAX*, and *PtaABCB* gene families in roots and internodes from 2-month-old plants, following exogenous IAA application, via qRT–PCR. *PtaPIN1*, *2*, and *7* and *PtaAUX5* and *6* were strongly upregulated in developing internodes, with *PtaPIN15* and *16* showing a more moderate increase (**Figure 9**). In contrast, *PtaPIN3* and *8* were strongly upregulated in roots, with *PtaAUX6* and *PtaABCB7* showing a lower expression level.

FIGURE 5 | Analysis of tissue-specific expression of *PIN, AUX/LAX,* and *ABCB* transcripts. Presence or absence of transcripts of genes coding for putative auxin transport proteins in the cortex, secondary phloem, cambial zone (i.e., initials and mother/daughter cells), and mature secondary xylem of *Populus tremula × alba* as determined by RT-PCR. Consensus of four biological replicates is shown, where GRAY = PRESENT, WHITE = ABSENT, and CROSS-HATCHED = VARIABLE among biological replicates. Samples were taken from the base of 6-month-old trees during active growth, approximately 100 internodes down from the top of the tree at a diameter of about 2 cm.

FIGURE 6 | Quantification of *PIN* transcripts expression by qRT-PCR. *PIN* genes show tissue-specific expression profiles that may reflect a role in directional auxin transport in developing vasculature, with *PtaPIN1* highly expressed across all tissues. *PtaPIN6, 7, 15,* and *16* were expressed in internodes and have not been described before. Total RNA was extracted from four biological replicates and qRT-PCR standard curves and assays were run in triplicate. Expression values were calculated via the $2^{-\Delta\Delta Ct}$ method (Livak and Schmittgen, 2001; Pfaffl, 2001) and baseline-corrected fluorescence values were normalized against the geometric mean of *PtaPD-E1, PtaTUA2, PtaUBQ, PtaACT2*. These reference genes were stably expressed across all tissues with the exception of developing xylem; this means that it is permissible to compare expression levels within any single tissue as well as across whole plantlets, internodes, and roots. Error bars represent the SEM.

DISCUSSION

THE ARRAY OF PUTATIVE AUXIN TRANSPORTERS IN *POPULUS* REFLECTS BOTH PRE-EXISTING DIVERSITY AND EXPANSION DUE TO GENOMIC AND SEGMENTAL DUPLICATIONS
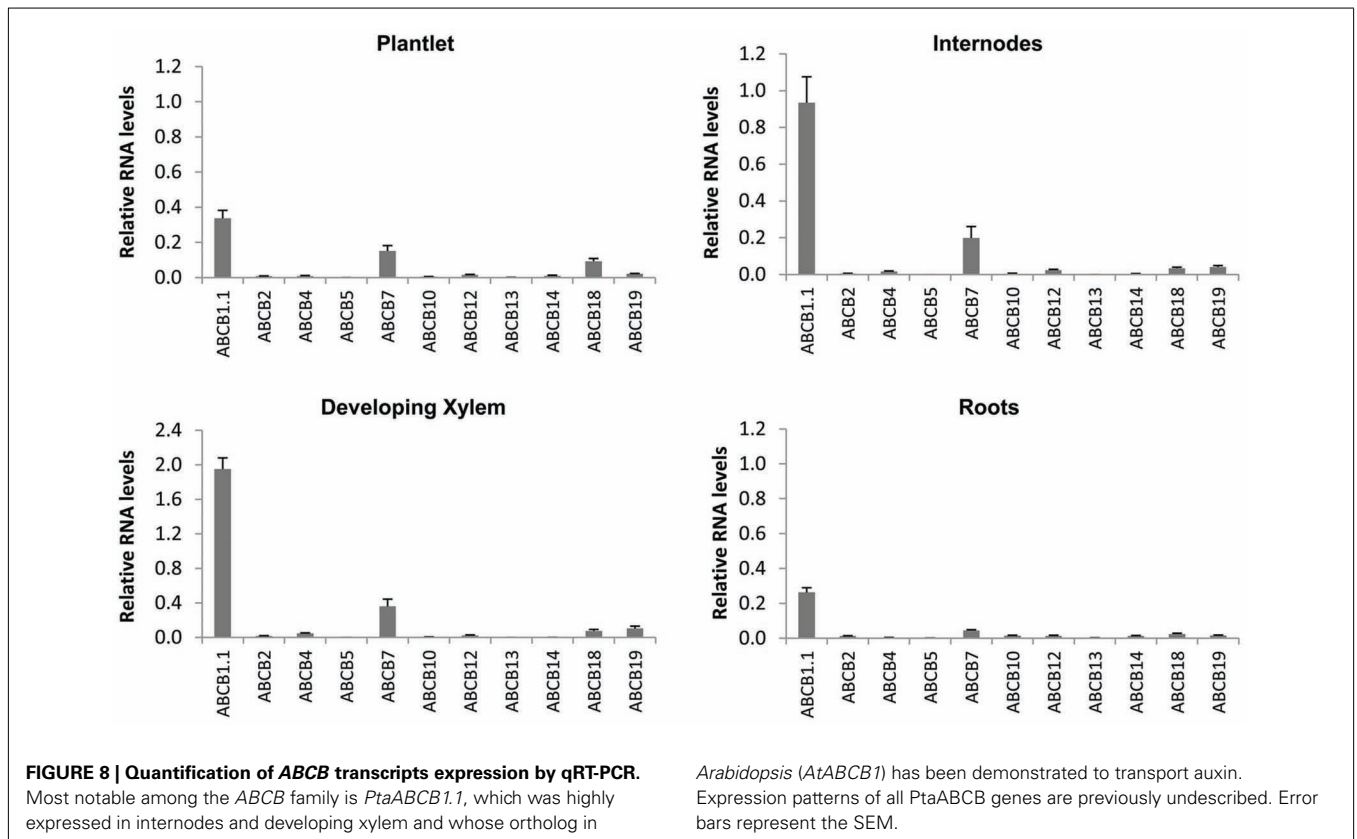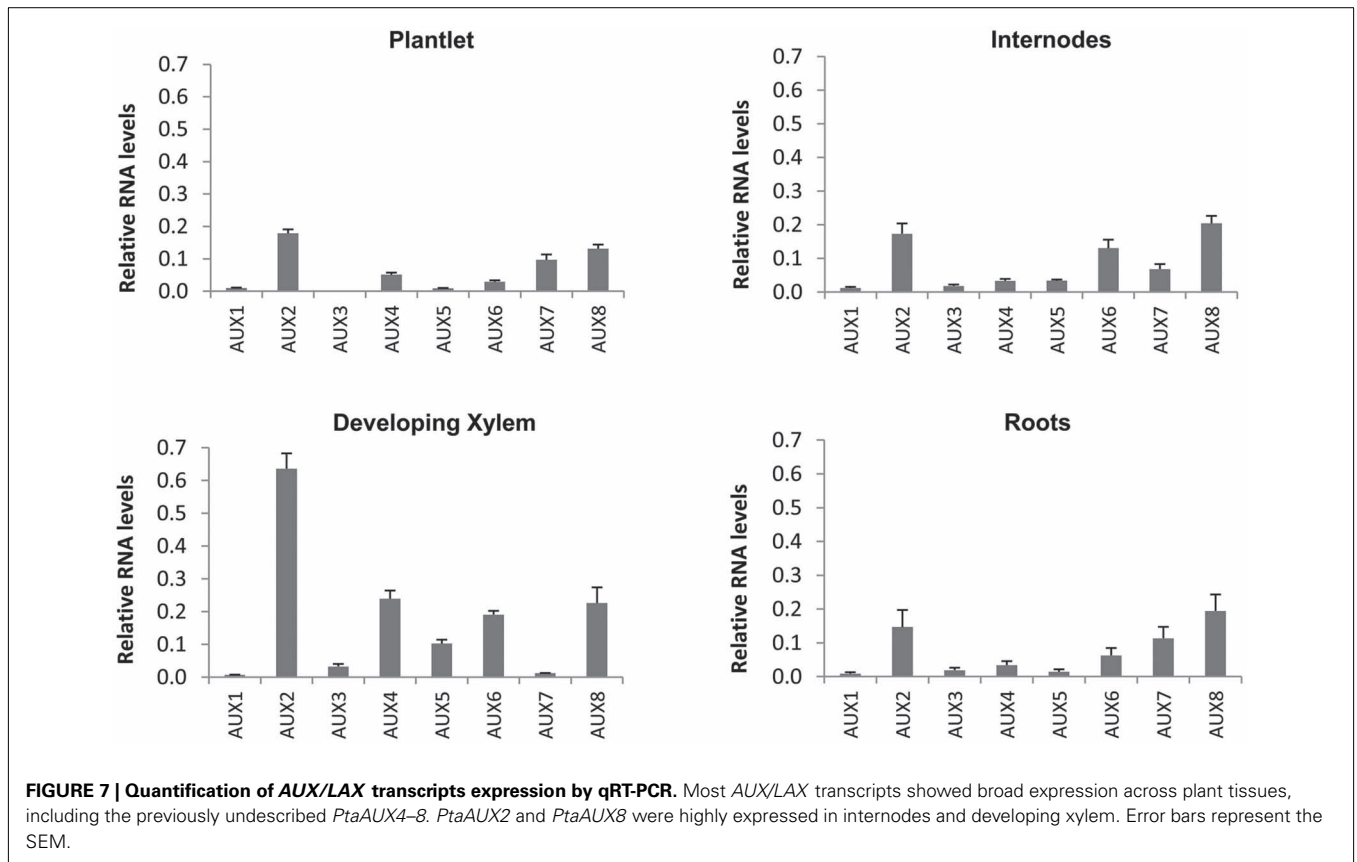
There are twice as many members of the *PIN* and *AUX/LAX* gene families in *Populus* as there are in *Arabidopsis* and both families show a number of clear pairs based on coding sequence (e.g., *PtrPIN4/5, PtrAUX3/4*; **Figures 2** and **3**). With no clear evidence for any tandem duplication in the *PIN* and *AUX/LAX* gene families, it is possible that all gene copies were retained following the "salicoid" genome duplication (Tuskan et al., 2006). Although the functional role of these proteins has not been demonstrated in *Populus*, given the conserved protein structure and known specificity for IAA for most PINs in *Arabidopsis* (and to a lesser extent, AUX/LAX proteins), it seems likely that they have retained a function in auxin transport. To what extent new PINs have developed specialized roles in PAT in *Populus* is not known and the added redundancy for such an important developmental mechanism may be beneficial enough to warrant retention. Indeed, redundancy in *Arabidopsis* allows single PIN mutants to complete embryogenesis, whereas quadruple mutants are required before severe defects are observed (Benková et al., 2003; Friml et al., 2003). At the same time it is interesting to note that there are clear differences in expression among presumed paralogs. For instance, *PtaPIN1* is expressed at much higher levels than *PtaPIN7* in internodes and developing xylem. Predictions about PIN function in *Populus* may also be
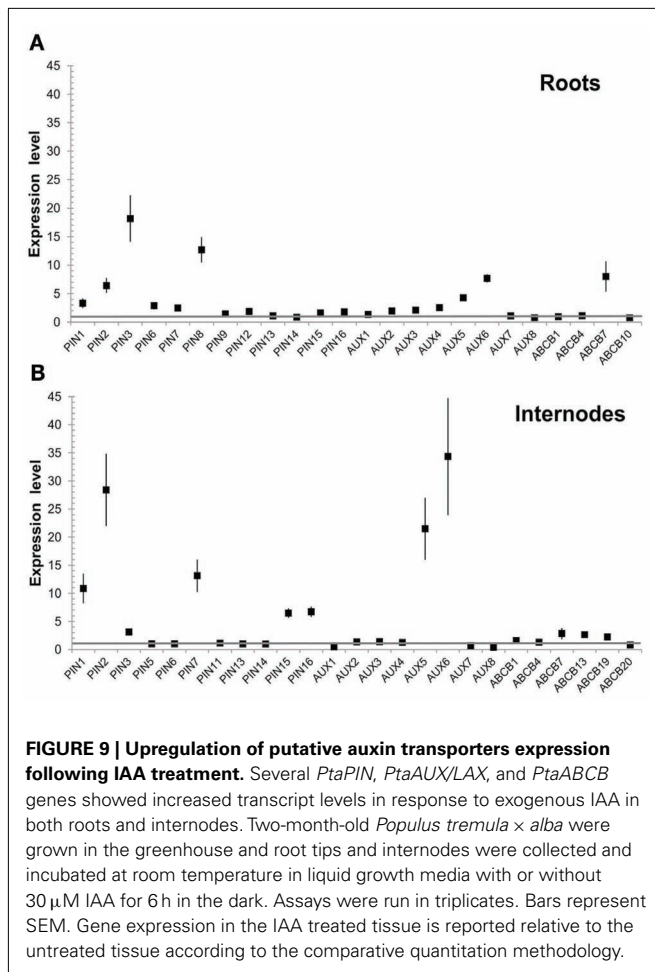
informed by structural comparisons with *Arabidopsis*. The "long" PINs in *Arabidopsis* are localized to the plasma membrane and function in PAT, whereas those with shorter structure are found in the ER (Mravec et al., 2009; Friml and Jones, 2010). PtrPIN1–3 and PtrPIN6–9 are all classified as "long" PINs (**Table A3** in Appendix), but it is not known whether similar localization patterns exist in *Populus*.

In contrast to the *PIN* and *AUX/LAX* gene families, the number of *ABCBs* in *Populus* is not expanded relative to *Arabidopsis* (both species include about 20 members; **Table A2** in Appendix) and only a few appear as closely related gene pairs. This is perhaps not surprising given that this gene family has a much deeper history and that ABCB proteins transport a number of substrates in addition to IAA. There also appears to be expansion in a number of angiosperms included in our phylogeny, such as *Z. mays, M. truncatula, P. persica,* and *Arabidopsis* (**Figure 4**). Although there has been retention of *ABCB* copies from both tandem duplication and whole genome duplication events in *Populus*, there also appears to have been loss. Much functional work is needed on *Populus* ABCB genes and proteins before any role in PAT can be ascribed.

CANDIDATE ABCBs FOR IAA TRANSPORT FUNCTION IN *POPULUS* ARE SUGGESTED BY PHYLOGENETIC PLACEMENT AND PROTEIN STRUCTURE PREDICTION

ATP-binding cassette proteins constitute a very large superfamily that has representatives across the bacteria, plant, and animal

FIGURE 7 | Quantification of *AUX/LAX* transcripts expression by qRT-PCR. Most *AUX/LAX* transcripts showed broad expression across plant tissues, including the previously undescribed *PtaAUX4–8*. *PtaAUX2* and *PtaAUX8* were highly expressed in internodes and developing xylem. Error bars represent the SEM.

FIGURE 8 | Quantification of *ABCB* transcripts expression by qRT-PCR.
Most notable among the *ABCB* family is *PtaABCB1.1*, which was highly expressed in internodes and developing xylem and whose ortholog in

Arabidopsis (*AtABCB1*) has been demonstrated to transport auxin. Expression patterns of all PtaABCB genes are previously undescribed. Error bars represent the SEM.

**FIGURE 9 | Upregulation of putative auxin transporters expression
following IAA treatment.** Several *PtaPIN*, *PtaAUX/LAX*, and *PtaABCB*
genes showed increased transcript levels in response to exogenous IAA in
both roots and internodes. Two-month-old *Populus tremula* × *alba* were
grown in the greenhouse and root tips and internodes were collected and
incubated at room temperature in liquid growth media with or without
30 μM IAA for 6 h in the dark. Assays were run in triplicates. Bars represent
SEM. Gene expression in the IAA treated tissue is reported relative to the
untreated tissue according to the comparative quantitation methodology.

kingdoms (Jasinski et al., 2003; Verrier et al., 2008) and, as a group,
are able to transport a wide array of different molecules (Geisler
et al., 2005; Bandyopadhyay et al., 2007). Among the ABCs, the sub-
class B includes proteins that are able to bind and transport auxin
across the plasma membrane in *Arabidopsis*, whereas other mem-
bers transport other substrates in addition to IAA (e.g., AtABCB14
functions primarily as a malate transporter (Lee et al., 2008)).
There has been no functional characterization of the ABCBs in
Populus to date and given the large size of the family and the
likely role of one or more members in IAA transport, we sought
to identify candidate PtrABCBs with this function. Our phylo-
genetic analysis shows that the coding sequences of *PtrABCB1.1*,
PtrABCB1.2, and *PtrABCB19* cluster together with *AtABCB1* and
AtABCB19 respectively, both of which are known IAA transporters
with high specificity for IAA (Zazímalová et al., 2010). Inter-
estingly, although 10 of the 20 PtaABCBs are predicted to have
one or more IAA binding sites based on tertiary structure, both
PtrABCB1 and PtrABCB19 have only one clearly defined binding
pocket for IAA. All but one of the remaining ABCBs with putative
IAA binding sites (PtrABCB2, PtrABCB5, PtrABCB6, PtrABCB8,
PtrABCB11, PtrABCB14) cluster together in the same clade, which
includes *AtABCB4*, a gene coding codes for another membrane
protein capable of IAA transport (Terasaka et al., 2005; Kubeš
et al., 2011). Similarly, *PtrABCB16* occurs in the same clade as

AtABCB13 and *AtABCB14*, where AtABCB14 has been recently
determined as responsible for auxin transport in the inflorescence
stem of *Arabidopsis* (Kaneda et al., 2011).

We found *PtrABCB1.1* to be highly expressed in most *Populus*
tissues, particularly in internodes and developing xylem. *PtrA-
BCB7* was also expressed in these same tissues and was strongly
upregulated in response to IAA, although most notably in roots.
However, although coding sequence similarity places *PtrABCB7*
as a close relative of a presumed IAA transporter in *Arabidopsis*
(AtABCB15; Kaneda et al., 2011), the protein was not predicted to
contain an IAA binding site. We suggest therefore that PtrABCB1.1
and its nearly identical paralog PtrABCB1.2 are the most logical
candidates for initial functional characterization, both in heterol-
ogous expression systems (e.g., *Schizosaccharomyces pombe*) and
in planta, given their phylogenetic placement relative to *AtABCB1*
and predicted IAA binding sites. It is interesting to note that in con-
trast to *AtABCB1* (Geisler et al., 2005), we did not find *PtaABCB1.1*
to be upregulated by exogenous IAA treatment. Lastly, we did not
observe strong expression of *PtaABCB19* in any *Populus* tissues
nor was it upregulated by IAA. The expression of its presumed
ortholog in *Arabidopsis*, *AtABCB19*, is induced by IAA treatments
(Noh et al., 2001) and the protein often co-localizes with AtPIN1
(Bandyopadhyay et al., 2007), suggesting that the relationship of
these two proteins may have changed. Clearly there is much to
be learned about the role of these ABCBs in IAA transport in
Populus.

AUXIN TRANSPORTERS IN *POPULUS* STEM DEVELOPMENT

That auxin regulates vascular development in woody plants is clear,
but our understanding of the genetic mechanisms and the role of
specific proteins in basipetal transport is limited. The expression of
PttPIN1–3 and *PttLAX1–3* has already been characterized in detail
across the developing stem tissues of *P. tremula* × *tremuloides*
(Schrader et al., 2003), but our results suggest that a far greater
number of putative transporters are expressed in young internodes
where cambial growth is being initiated. In particular, *PtaPIN1*,
PtaPIN6, and *PtaABCB1.1* are highly expressed in internodes, a
complex tissue that includes primary xylem parenchyma, primary
phloem, cortex, and a nascent vascular cambium. In developing
xylem, *PtaPIN1*, *PtaAUX2*, and *PtaABCB1.1* are highly expressed,
with the latter likely to function in auxin transport given its
protein sequence similarity to *AtABCB1*. Similarly, several pre-
viously uncharacterized transporters are strongly upregulated by
auxin, including *PtaPIN8*, *PtaAUX6*, and *PtaABCB7* in roots and
PtaPIN7, *PtaPIN15*, *PtaPIN16*, *PtaAUX5*, and *PtaAUX6* in intern-
odes. Given the retention of copies of auxin transporters following
duplication events, there is likely to be both redundancy and
neo-functionalization for PAT proteins in *Populus*.

The vascular cambium and the secondary xylem and phloem
that it produces are often viewed as distinct from primary growth,
but it is important to remember that vascular development forms
a continuum between stem and leaf (Spicer and Groover, 2010).
We know a great deal about the role of PAT in venation pattern-
ing in leaves of *Arabidopsis* (Scarpella et al., 2006). Here, AtPIN1
directs auxin flow up through the epidermis toward a conver-
gence point, from where it is channeled down through the center
of a developing leaf primordium, establishing the location of the

first central vascular bundle. This vascular bundle differentiates from a strand of procambium that is continuous with the vascular cambium below, such that the basipetal transport of auxin out of developing primordia is likely continuous with the basipetal stream moving down through the cambium (Lachaud and Bonnemain, 1984; Uggla et al., 1998; Kramer et al., 2008). Based on a combination of our results and published work in both *Arabidopsis* and *Populus*, we suggest that PtaPIN1, PtaAUX2, and PtaABCB1.1 are the best initial candidates for the maintenance of PAT in the cambial zone, although additional transporters are very likely involved. Given the slow time course and laborious nature of transformation in woody plants, our hope is that this work will provide a starting point for work in planta by identifying candidate IAA transporters involved in woody stem development. Functional studies, transport assays and protein localization are all needed to resolve the action of specific transporters in shaping the distribution of auxin across the cambial zone.

Finally, it is interesting to note that several members of the *PIN*, *AUX/LAX*, and *ABCB* gene families are expressed in the mature xylem. Although the bulk of this tissue is dead (e.g., vessels and fibers), ray parenchyma cells remain alive for many years (Spicer and Holbrook, 2007) and serve as a route of transport between xylem and phloem (Van Bel, 1990). In particular, *PtaPIN1*, *PtaAUX2*, *PtaAUX3*, *PtaAUX4* and *PtaABCB1*, *PtaABCB7*, *PtaABCB20* were found to be expressed in these cells. In addition to their role in carbohydrate transport and storage, xylem parenchyma cells are able to exchange solutes with the transpiration stream and function in wound response. What is puzzling however is that these cells are symplasmically connected, at least in the radial direction, whereas PAT requires transport across a membrane. Furthermore, there is no evidence for free IAA in mature xylem (Uggla et al., 1996; Tuominen et al., 1997). Although conjugated forms of IAA are transported in the phloem (Baker, 2000) no studies to date have looked for conjugated IAA in ray or axial parenchyma in secondary xylem. Given their role in wound response, some capacity for IAA transport (or even IAA synthesis) would not be surprising, but transport assays and protein localization are needed to clarify any potential role these cells might play in IAA transport.

THE *ABCB* GENE FAMILY DIVERSIFIED PRIOR TO THE *PIN* AND *AUX/LAX* FAMILIES AND PRIOR TO THE DIVERSIFICATION OF LAND PLANTS

It is clear from our phylogenetic analysis that the *ABCB* gene family existed before the diversification of land plants, whereas the *PIN* and *AUX/LAX* families arose within the land plant clade. This is supported by the fact that *ABCB* genes from a moss (*P. patens*) and a lycopod (*S. moellendorffii*) consistently occur nested within multiple, well-supported clades that also include higher plants (**Figure 4**; **Figure A3** in Appendix). It also confirms previous work reconstructing the evolutionary history of this family (Bandyopadhyay et al., 2007; Krecek et al., 2009). In contrast, diversification of

the *PIN* and *AUX/LAX* gene families occurred after the origin of land plants, as suggested by the well-supported and exclusively basal position of both *Physcomitrella* and *Selaginella PIN* and *AUX/LAX* genes (**Figures 2** and **3**). There was already considerable diversity in the *ABCB* gene family at the time of the monocot/dicot divergence, dated at approximately 130–150 Myr ago (Wolfe et al., 1989; Chaw et al., 2004; Bell et al., 2010), as we recovered as many as 10 distinct *ABCB* gene clades that contain a clear monocot/dicot split with strong support. The picture is not as clear for the *PIN* and *AUX/LAX* genes due to weak support at some nodes, but there may have been five copies of the *PIN* and likely just two copies of the *AUX/LAX* genes at the time of the monocot/dicot divergence. It is not clear at this time whether all *AUX/LAX* genes in monocots descended from a single original copy, as suggested by the tree found using aligned sequences under parsimony, since monocot *AUX/LAX* genes were not recovered in a single clade in other trees (**Figure 3**).

In conclusion, we show that the deep history of the ABCB family of transporters coupled with the expansion of the PIN and AUX/LAX families following a genome duplication has led to a diverse array of over 40 putative auxin transport proteins in *Populus*. Given this large number and the inherent difficulties in working with a woody plant (e.g., long generation times, slow transformation process, difficult nucleic acid extraction), it is important to establish a comprehensive picture of gene expression profiles and predict their protein structures. By considering both evolutionary relationships and structural similarities to known auxin transporters, we can choose the most appropriate candidates for future study. One of the main goals in the short term should be to develop a set of tools for protein localization, including antibodies and protein fusions for stable plant transformation. Although technically difficult for trees, these findings should be coupled with functional studies with knockout mutants. Lastly, it will be important to determine the transport capacity and substrate specificity of target proteins of *Populus* by expressing them in heterologous systems such as *S. pombe*. We hope that this work provides a foundation on which to build an improved understanding of auxin transport in *Populus*, as knowing the role of specific transport proteins in secondary vascular development is likely key to enhanced utilization of woody plants.

REFERENCES

Bainbridge, K., Guyomarc'h, S., Bayer, E., Swarup, R., Bennett, M., Mandel, T., and Kuhlemeier, C. (2008). Auxin influx carriers stabilize phyllotactic patterning. *Genes Dev.* 22, 810–823.

Baker, D. A. (2000). Long-distance vascular transport of endogenous hormones in plants and their role in source: sink regulation. *Isr. J. Plant Sci.* 48, 199–203.

Bandyopadhyay, A., Blakeslee, J. J., Lee, O. R., Mravec, J., Sauer, M., Titapiwatanakun, B., Makam, S. N.,

Bouchard, R., Geisler, M., Martinoia, E., Friml, J., Peer, W. A., and Murphy, A. S. (2007). Interactions of PIN and PGP auxin transport mechanisms. *Biochem. Soc. Trans.* 35, 137–141.

Banks, J. A., Nishiyama, T., Hasebe, M., Bowman, J. L., Gribskov, M., DePamphilis, C., Albert, V. A., Aono, N., Aoyama, T., Ambrose, B. A., Ashton, N. W., Axtell, M. J., Barker, E., Barker, M. S., Bennetzen, J. L., Bonawitz, N. D., Chapple, C., Cheng, C., Correa, L. G., Dacre, M., DeBarry, J., Dreyer, I., Elias, M., Engstrom, E. M., Estelle, M., Feng, L., Finet, C., Floyd, S. K., Frommer, W. B., Fujita, T., Gramzow, L., Gutensohn, M., Harholt, J., Hattori, M., Heyl, A., Hirai, T., Hiwatashi, Y., Ishikawa, M., Iwata, M., Karol, K. G., Koehler, B., Kolukisaoglu, U., Kubo, M., Kurata, T., Lalonde, S., Li, K., Li, Y., Litt, A., Lyons, E., Manning, G., Maruyama, T., Michael, T. P., Mikami, K., Miyazaki, S., Morinaga, S., Murata, T., Mueller-Roeber, B., Nelson, D. R., Obara, M., Oguri, Y., Olmstead, R. G., Onodera, N., Petersen, B. L., Pils, B., Prigge, M., Rensing, S. A., Riaño-Pachón, D. M., Roberts, A. W., Sato, Y., Scheller, H. V., Schulz, B., Schulz, C., Shakirov, E. V., Shibagaki, N., Shinohara, N., Shippen, D. E., Sørensen, I., Sotooka, R., Sugimoto, N., Sugita, M., Sumikawa, N., Tanurdzic, M., Theissen, G., Ulvskov, P., Wakazuki, S., Weng, J. K., Willats, W. W., Wipf, D., Wolf, P. G., Yang, L., Zimmer, A. D., Zhu, Q., Mitros, T., Hellsten, U., Loqué, D., Otillar, R., Salamov, A., Schmutz, J., Shapiro, H., Lindquist, E., Lucas, S., Rokhsar, D., and Grigoriev, I. V. (2011). The *Selaginella* genome identifies genetic changes associated with the evolution of vascular plants. *Science* 332, 960–963.

Bell, C. D., Soltis, D. E., and Soltis, P. S. (2010). The age and diversification of the angiosperms re-revisited. *Am. J. Bot.* 97, 1296–1303.

Benková, E., Michniewicz, M., Sauer, M., Teichmann, T., Seifertová, D., Jürgens, G., and Friml, J. (2003). Local, efflux-dependent auxin gradients as a common module for plant organ formation. *Cell* 115, 591–602.

Bennett, M. J., Marchant, A., Green, H. G., May, S. T., Ward, S. P., Millner, P. A., Walker, A. R., Schulz, B., and Feldmann, K. A. (1996). *Arabidopsis* AUX1 gene: a permease-like regulator of root gravitropism. *Science* 273, 948–950.

Björklund, S., Antti, H., Uddestrand, I., Moritz, T., and Sundberg, B. (2007). Cross-talk between gibberellin and auxin in development of Populus wood: gibberellin stimulates polar auxin transport and has a common transcriptome with auxin. *Plant J.* 52, 499–511.

Brunner, A. M., Yakovlev, I. A., and Strauss, S. H. (2004). Validating internal controls for quantitative plant gene expression studies. *BMC Plant Biol.* 4, 14. doi:10.1186/1471-2229-4-14

Carraro, N., Forestan, C., Canova, S., Traas, J., and Varotto, S. (2006). ZmPIN1a and ZmPIN1b encode two novel putative candidates for polar auxin transport and plant architecture determination of maize. *Plant Physiol.* 142, 254–264.

Castresana, J. (2000). Selection of conserved blocks from multiple alignments for their use in phylogenetic analysis. *Mol. Biol. Evol.* 17, 540–552.

Chaw, S.-M., Chang, C.-C., Chen, H.-L., and Li, W.-H. (2004). Dating the monocot-dicot divergence and the origin of core eudicots using whole chloroplast genomes. *J. Mol. Evol.* 58, 424–441.

Chen, R., Hilson, P., Sedbrook, J., Rosen, E., Caspar, T., and Masson, P. H. (1998). The *Arabidopsis thaliana* AGRAVITROPIC 1 gene encodes a component of the polar-auxin-transport efflux carrier. *Proc. Natl. Acad. Sci. U.S.A.* 95, 15112–15117.

Dolinsky, T. J., Czodrowski, P., Li, H., Nielsen, J. E., Jensen, J. H., Klebe, G., and Baker, N. A. (2007). PDB2PQR: expanding and upgrading automated preparation of biomolecular structures for molecular simulations. *Nucleic Acids Res.* 35, W522–W525.

Dolinsky, T. J., Nielsen, J. E., McCammon, J. A., and Baker, N. A. (2004). PDB2PQR: an automated pipeline for the setup of Poisson-Boltzmann electrostatics calculations. *Nucleic Acids Res.* 32, W665–W667.

Forestan, C., Meda, S., and Varotto, S. (2010). ZmPIN1-mediated auxin transport is related to cellular differentiation during maize embryogenesis and endosperm development. *Plant Physiol.* 152, 1373–1390.

Friml, J., Benková, E., Blilou, I., Wisniewska, J., Hamann, T., Ljung, K., Woody, S., Sandberg, G., Scheres, B., Jürgens, G., and Palme, K. (2002a). AtPIN4 mediates sink-driven auxin gradients and root patterning in *Arabidopsis*. *Cell* 108, 661–673.

Friml, J., Wisniewska, J., Benková, E., Mendgen, K., and Palme, K. (2002b). Lateral relocation of auxin efflux regulator PIN3 mediates tropism in *Arabidopsis*. *Nature* 415, 806–809.

Friml, J., and Jones, A. R. (2010). Endoplasmic reticulum: the rising compartment in auxin biology. *Plant Physiol.* 154, 458–462.

Friml, J., Vieten, A., Sauer, M., Weijers, D., Schwarz, H., Hamann, T., Offringa, R., and Jürgens, G. (2003). Efflux-dependent auxin gradients establish the apical-basal axis of *Arabidopsis*. *Nature* 426, 147–153.

Gälweiler, L., Guan, C., Müller, A., Wisman, E., Mendgen, K., Yephremov, A., and Palme, K. (1998). Regulation of polar auxin transport by AtPIN1 in *Arabidopsis* vascular tissue. *Science* 282, 2226–2230.

Geisler, M., Blakeslee, J. J., Bouchard, R., Lee, O. R., Vincenzetti, V., Bandyopadhyay, A., Titapiwatanakun, B., Peer, W. A., Bailly, A., Richards, E. L., Ejendal, K. F., Smith, A. P., Baroux, C., Grossniklaus, U., Müller, A., Hrycyna, C. A., Dudler, R., Murphy, A. S., and Martinoia, E. (2005). Cellular efflux of auxin catalyzed by the *Arabidopsis* MDR/PGP transporter AtPGP1. *Plant J.* 44, 179–194.

Guo, A.-Y., Zhu, Q.-H., Chen, X., and Luo, J.-C. (2007). GSDS: a gene structure display server. *Yi Chuan* 29, 1023–1026.

Gutierrez, L., Mauriat, M., Guénin, S., Pelloux, J., Lefebvre, J.-F., Louvet, R., Rusterucci, C., Moritz, T., Guerineau, F., Bellini, C., and Van Wuytswinkel, O. (2008). The lack of a systematic validation of reference genes: a serious pitfall undervalued in reverse transcription-polymerase chain reaction (RT-PCR) analysis in plants. *Plant Biotechnol. J.* 6, 609–618.

Hellgren, J. M., Olofsson, K., Plant, U., Centre, S., and Sciences, A. (2004). Patterns of auxin distribution during gravitational induction of reaction wood in poplar and pine. *Plant Physiol.* 135, 212–220.

Jasinski, M., Ducos, E., Martinoia, E., and Boutry, M. (2003). The ATP-binding cassette transporters: structure, function, and gene family comparison between. *Plant Physiol.* 131, 1169–1177.

Kaneda, M., Schuetz, M., Lin, B. S. P., Chanis, C., Hamberger, B., Western, T. L., Ehlting, J., and Samuels, A, L. (2011). ABC transporters coordinately expressed during lignification of *Arabidopsis* stems include a set of ABCBs associated with auxin transport. *J. Exp. Bot.* 62, 2063–2077.

Katekar, G. F., and Geissler, A. E. (1980). Auxin transport inhibitors. *Plant Physiol.* 66, 1190–1195.

Katoh, K., Asimenos, G., and Toh, H. (2009). Multiple alignment of DNA sequences with MAFFT. *Methods Mol. Biol.* 537, 39–64.

Knöller, A. S., Blakeslee, J. J., Richards, E. L., Peer, W. A., and Murphy, A. S. (2010). Brachytic2/ZmABCB1 functions in IAA export from intercalary meristems. *J. Exp. Bot.* 61, 3689–3696.

Kramer, E. M., Dorit, R. L., and Irish, V. F. (1998). Molecular evolution of genes controlling petal and stamen development: duplication and divergence within the APETALA3 and PISTILLATA MADS-box gene lineages. *Genetics* 149, 765–783.

Kramer, E. M., Lewandowski, M., Beri, S., Bernard, J., Borkowski, M., Borkowski, M. H., Burchfield, L. A., Mathisen, B., and Normanly, J. (2008). Auxin gradients are associated with polarity changes in trees. *Science* 320, 1610.

Kubeš, M., Yang, H., Richter, G. L., Cheng, Y., Mlodzinska, E., Wang, X., Blakeslee, J. J., Carraro, N., Petrášek, J., Zažímalová, E., Hoyerová, K., Peer, W. A., and Murphy, A. S. (2011). The *Arabidopsis* concentration-dependent influx/efflux transporter ABCB4 regulates cellular auxin levels in the root epidermis. *Plant J.* [Epub ahead of print].

Krecek, P., Skupa, P., Libus, J., Naramoto, S., Tejos, R., Friml, J., and Zažímalová, E. (2009). Protein family review The PIN-FORMED (PIN) protein family of auxin transporters. *Genome Biol.* 10, 1–11.

Lachaud, S., and Bonnemain, J. L. (1984). Seasonal variations in the polar transport pathways and retention sites of [^{3}H]indole-3-acetic acid in young branches of *Fagus sylvatica* L. *Planta* 161, 207–215.

Lee, B. H. A., Johnston, R., Yang, Y., Gallavotti, A., Kojima, M., Travençolo, B. A. N., Costa, L. D. F., Sakakibara, H., and Jackson, D. (2009). Studies of aberrant phyllotaxy1 mutants of maize indicate complex interactions between auxin and cytokinin signaling in the shoot apical meristem. *Plant Physiol.* 150, 205–216.

Lee, M., Choi, Y., Burla, B., Kim, Y.-Y., Jeon, B., Maeshima, M., Yoo, J.-Y., Martinoia, E., and Lee, Y. (2008). The ABC transporter AtABCB14 is a malate importer and modulates stomatal response to CO2. *Nat. Cell Biol.* 10, 1217–1223.

Livak, K. J., and Schmittgen, T. D. (2001). Analysis of relative gene expression data using real-time quantitative PCR and the 2(-Delta Delta C(T)) method. *Methods* 25, 402–408.

Ljung, K., Bhalerao, R. P., and Sandberg, G. (2001a). Sites and homeostatic control of auxin biosynthesis in *Arabidopsis* during vegetative growth. *Plant J.* 28, 465–474.

Ljung, K., Ostin, A., Lioussanne, L., and Sandberg, G. (2001b). Developmental regulation of indole-3-acetic acid turnover in Scots pine seedlings. *Plant Physiol.* 125, 464–475.

Ljung, K., Hull, A. K., Celenza, J., Yamada, M., Estelle, M., and Normanly, J. (2005). Sites and regulation of auxin biosynthesis in *Arabidopsis* roots. *Plant Cell* 17, 1090–1104.

Lomax, T., Muday, G. K., and Rubery, P. H. (1995). *Plant Hormones: Physiology, Biochemistry, and Molecular Biology.* Dordrecht: K. A. Publishers.

Luschnig, C., Gaxiola, R. A., Grisafi, P., and Fink, G. R. (1998). EIR1, a root-specific protein involved in auxin transport, is required for gravitropism in *Arabidopsis thaliana. Genes Dev.* 12, 2175–2187.

Merchant, S. S., Prochnik, S. E., Vallon, O., Harris, E. H., Karpowicz, S. J., Witman, G. B., Terry, A., Salamov, A., Fritz-Laylin, L. K., Maréchal-Drouard, L., Marshall, W. F., Qu, L. H., Nelson, D. R., Sanderfoot, A. A., Spalding, M. H., Kapitonov, V. V., Ren, Q., Ferris, P., Lindquist, E., Shapiro, H., Lucas, S. M., Grimwood, J., Schmutz, J., Cardol, P., Cerutti, H., Chanfreau, G., Chen, C. L., Cognat, V., Croft, M. T., Dent, R., Dutcher, S., Fernández, E., Fukuzawa, H., González-Ballester, D., González-Halphen, D., Hallmann, A., Hanikenne, M., Hippler, M., Inwood, W., Jabbari, K., Kalanon, M., Kuras, R., Lefebvre, P. A., Lemaire, S. D., Lobanov, A. V., Lohr, M., Manuell, A., Meier, I., Mets, L., Mittag, M., Mittelmeier, T., Moroney, J. V., Moseley, J., Napoli, C., Nedelcu, A. M., Niyogi, K., Novoselov, S. V., Paulsen, I. T., Pazour, G., Purton, S., Ral, J. P., Riaño-Pachón, D. M., Riekhof, W., Rymarquis, L., Schroda, M., Stern, D., Umen, J., Willows, R., Wilson, N., Zimmer, S. L., Allmer, J., Balk, J., Bisova, K., Chen, C. J., Elias, M., Gendler, K., Hauser, C., Lamb, M. R., Ledford, H., Long, J. C., Minagawa, J., Page, M. K., Pan, J., Pootakham, W., Roje, S., Rose, A., Stahlberg, E., Terauchi, A. M., Yang, P., Ball, S., Bowler, C., Dieckmann, C. L., Gladyshev, V. N., Green, P., Jorgensen, R., Mayfield, S., Mueller-Roeber, B., Rajamani, S., Sayre, R. T., Brokstein, P., Dubchak, I., Goodstein, D., Hornick, L., Huang, Y. W., Jhaveri, J., Luo, Y., Martínez, D., Ngau, W. C., Otillar, B., Poliakov, A., Porter, A., Szajkowski, L., Werner, G., Zhou, K., Grigoriev, I. V., Rokhsar, D. S., and Grossman, A. R. (2007). The *Chlamydomonas* genome reveals the evolution of key animal and plant functions. *Science* 318, 245–250.

Miller, M. A., Pfeiffer, W., and Schwartz, T. (2010). "Creating the CIPRES science gateway for inference of large phylogenetic trees," in *Gateway Computing Environments Workshop (GCE)*, New Orleans.

Mravec, J., Skupa, P., Bailly, A., Hoyerová, K., Krecek, P., Bielach, A., Petrásek, J., Zhang, J., Gaykova, V., Stierhof, Y.-D., Dobrev, P. I., Schwarzerová, K., Rolcík, J., Seifertová, D., Luschnig, C., Benková, E., Zazímalová, E., Geisler, M., and Friml, J. (2009). Subcellular homeostasis of phytohormone auxin is mediated by the ER-localized PIN5 transporter. *Nature* 459, 1136–1140.

Müller, A., Guan, C., Gälweiler, L., Tänzler, P., Huijser, P., Marchant, A., Parry, G., Bennett, M., Wisman, E., and Palme, K. (1998). AtPIN2 defines a locus of *Arabidopsis* for root gravitropism control. *EMBO J.* 17, 6903–6911.

Multani, D. S., Briggs, S. P., Chamberlin, M. A, Blakeslee, J. J., Murphy, A. S., and Johal, G. S. (2003). Loss of an MDR transporter in compact stalks of maize br2 and sorghum dw3 mutants. *Science* 302, 81–84.

Nilsson, J., Karlberg, A., Antti, H., Lopez-Vernaza, M., Mellerowicz, E., Perrot-Rechenmann, C., Sandberg, G., and Bhalerao, R. P. (2008). Dissecting the molecular basis of the regulation of wood formation by auxin in hybrid aspen. *Plant Cell* 20, 843–855.

Noh, B., Murphy, A. S., and Spalding, E. P. (2001). Multidrug resistance-like genes of *Arabidopsis* required for auxin transport and auxin-mediated development. *Plant Cell* 13, 2441–2454.

Okada, K., Ueda, J., Komaki, M. K., Bell, C. J., and Shimura, Y. (1991). Requirement of the auxin polar transport system in early stages of *Arabidopsis* floral bud formation. *Plant Cell* 3, 677.

Petrásek, J., and Friml, J. (2009). Auxin transport routes in plant development. *Development* 136, 2675–2688.

Pfaffl, M. W. (2001). A new mathematical model for relative quantification in real-time RT-PCR. *Nucleic Acids Res.* 29, e45.

Prochnik, S. E., Umen, J., Nedelcu, A. M., Hallmann, A., Miller, S. M., Nishii, I., Ferris, P., Kuo, A., Mitros, T., Fritz-Laylin, L. K., Hellsten, U., Chapman, J., Simakov, O., Rensing, S. A., Terry, A., Pangilinan, J., Kapitonov, V., Jurka, J., Salamov, A., Shapiro, H., Schmutz, J., Grimwood, J., Lindquist, E., Lucas, S., Grigoriev, I. V., Schmitt, R., Kirk, D., and Rokhsar, D. S. (2010). Genomic analysis of organismal complexity in the multicellular green alga *Volvox carteri. Science* 329, 223–226.

Rea, P. A. (2007). Plant ATP-binding cassette transporters. *Annu. Rev. Plant Biol.* 58, 347–375.

Rensing, S. A., Lang, D., Zimmer, A. D., Terry, A., Salamov, A., Shapiro, H., Nishiyama, T., Perroud, P.-F., Lindquist, E. A., Kamisugi, Y., Tanahashi, T., Sakakibara, K., Fujita, T., Oishi, K., Shin-I, T., Kuroki, Y., Toyoda, A., Suzuki, Y., Hashimoto, S., Yamaguchi, K., Sugano, S., Kohara, Y., Fujiyama, A., Anterola, A., Aoki, S., Ashton, N., Barbazuk, W. B., Barker, E., Bennetzen, J. L., Blankenship, R., Cho, S. H., Dutcher, S. K., Estelle, M., Fawcett, J. A., Gundlach, H., Hanada, K., Heyl, A., Hicks, K. A., Hughes, J., Lohr, M., Mayer, K., Melkozernov, A., Murata, T., Nelson, D. R., Pils, B., Prigge, M., Reiss, B., Renner, T., Rombauts, S., Rushton, P. J., Sanderfoot, A., Schween, G., Shiu, S. H., Stueber, K., Theodoulou, F. L., Tu, H., Van de Peer, Y., Verrier, P. J., Waters, E., Wood, A., Yang, L., Cove, D., Cuming, A. C., Hasebe, M., Lucas, S., Mishler, B. D., Reski, R., Grigoriev, I. V., Quatrano, R. S., and Boore, J. L. (2008). The *Physcomitrella* genome reveals evolutionary insights into the conquest of land by plants. *Science* 319, 64–69.

Sanchez-Fernandez, R., Davies, T. G., Coleman, J. O., and Rea, P. A. (2001). The *Arabidopsis thaliana* ABC protein superfamily, a complete inventory. *J. Biol. Chem.* 276, 30231–30244.

Sauer, M., Balla, J., Luschnig, C., Wisniewska, J., Reinöhl, V., Friml, J., and Benková, E. (2006). Canalization of auxin flow by Aux/IAA-ARF-dependent feedback regulation of PIN polarity. *Genes Dev.* 20, 2902–2911.

Scarpella, E., Marcos, D., Friml, J., and Berleth, T. (2006). Control of leaf vascular patterning by polar auxin transport. *Genes Dev.* 20, 1015–1027.

Schrader, J., Baba, K., May, S. T., Palme, K., Bennett, M., Bhalerao, R. P., and Sandberg, G. (2003). Polar auxin transport in the wood-forming tissues of hybrid aspen is under simultaneous control of developmental and environmental signals. *Proc. Natl. Acad. Sci. U.S.A.* 100, 10096–10101.

Schrader, J., Moyle, R., Bhalerao, R., Hertzberg, M., Lundeberg, J., Nilsson, P., and Bhalerao, R. P. (2004). Cambial meristem dormancy in trees involves extensive remodelling of the transcriptome. *Plant J.* 40, 173–187.

Secchi, F., MacIver, B., Zeidel, M. L., and Zwieniecki, M. A. (2009). Functional analysis of putative genes encoding the PIP2 water channel subfamily in *Populus trichocarpa. Tree Physiol.* 29, 1467–1477.

Shen, C., Bai, Y., Wang, S., Zhang, S., Wu, Y., Chen, M., Jiang, D., and Qi, Y. (2010). Expression profile of PIN, AUX/LAX and PGP auxin transporter gene families in *Sorghum bicolor* under phytohormone and abiotic stress. *FEBS J.* 277, 2954–2969.

Sidler, M., Hassa, P., Hasan, S., Ringli, C., and Dudler, R. (1998). Involvement of an ABC transporter in a developmental pathway regulating hypocotyl cell elongation in the light. *Plant Cell* 10, 1623–1636.

Spicer, R., and Groover, A. (2010). Evolution of development of vascular cambia and secondary growth. *New Phytol.* 186, 577–592.

Spicer, R., and Holbrook, N. M. (2007). Parenchyma cell respiration and survival in secondary xylem: does metabolic activity decline with cell age? *Plant Cell Environ.* 30, 934–943.

Stamatakis, A., Hoover, P., and Rougemont, J. (2008). A rapid bootstrap algorithm for the RAxML Web servers. *Syst. Biol.* 57, 758–771.

Sussman, M. R., and Goldsmith, M. H. M. (1981). The action of specific inhibitors of auxin transport on uptake of auxin and binding of N-1-naphthylphthalamic acid to a membrane site in maize coleoptiles. *Planta* 13–18.

Swarup, K., Benková, E., Swarup, R., Casimiro, I., Péret, B., Yang, Y., Parry, G., Nielsen, E., De Smet, I., Vanneste, S., Levesque, M. P., Carrier, D., James, N., Calvo, V., Ljung, K., Kramer, E., Roberts, R., Graham, N., Marillonnet, S., Patel, K., Jones, J. D., Taylor, C. G., Schachtman, D. P., May, S., Sandberg, G., Benfey, P., Friml, J., Kerr, I., Beeckman, T., Laplaze, L., and Bennett, M. J. (2008). The auxin influx carrier LAX3 promotes lateral root emergence. *Nat. Cell Biol.* 10, 946–954.

Swarup, R., Friml, J., Marchant, A., Ljung, K., Sandberg, G., Palme, K., and Bennett, M. (2001). Localization of the auxin permease AUX1 suggests two functionally distinct hormone transport pathways operate in the *Arabidopsis* root apex. *Genes Dev.* 15, 2648–2653.

Swarup, R., Kramer, E. M., Perry, P., Knox, K., Leyser, H. M. O., Haseloff, J., Beemster, G. T. S., Bhalerao, R., and Bennett, M. J. (2005). Root gravitropism requires lateral root cap and epidermal cells for transport and response to a mobile auxin signal. *Nat. Cell Biol.* 7, 1057–1065.

Talavera, G., and Castresana, J. (2007). Improvement of phylogenies after removing divergent and ambiguously aligned blocks from protein sequence alignments. *Syst. Biol.* 56, 564–577.

Terasaka, K., Blakeslee, J. J., Titapiwatanakun, B., Peer, W. A., Bandyopadhyay, A., Makam, S. N., Lee, R., Richards, E. L., Murphy, A. S., Sato, F., and Yazaki, K. (2005). PGP4, an ATP binding cassette P-glycoprotein, catalyzes auxin transport in *Arabidopsis thaliana* roots. *Plant Cell* 17, 2922–2939.

Titapiwatanakun, B., and Murphy, A. S. (2009). Post-transcriptional regulation of auxin transport proteins: cellular trafficking, protein phosphorylation, protein maturation, ubiquitination, and membrane composition. *J. Exp. Bot.* 60, 1093–1107.

Tuominen, H., Puech, L., Fink, S., and Sundberg, B. (1997). A radial concentration gradient of indole-3-acetic acid is related to secondary xylem development in hybrid aspen. *Plant Physiol.* 115, 577–585.

Tuskan, G. A., Difazio, S., Jansson, S., Bohlmann, J., Grigoriev, I., Hellsten, U., Putnam, N., Ralph, S., Rombauts, S., Salamov, A., Schein, J., Sterck, L., Aerts, A., Bhalerao, R. R., Bhalerao, R. P., Blaudez, D., Boerjan, W., Brun, A., Brunner, A., Busov, V., Campbell, M., Carlson, J., Chalot, M., Chapman, J., Chen, G. L., Cooper, D., Coutinho, P. M., Couturier, J., Covert, S., Cronk, Q., Cunningham, R., Davis, J., Degroeve, S., Déjardin, A., Depamphilis, C., Detter, J., Dirks, B., Dubchak, I., Duplessis, S., Ehlting, J., Ellis, B., Gendler, K., Goodstein, D., Gribskov, M., Grimwood, J., Groover, A., Gunter, L., Hamberger, B., Heinze, B., Helariutta, Y., Henrissat, B., Holligan, D., Holt, R., Huang, W., Islam-Faridi, N., Jones, S., Jones-Rhoades, M., Jorgensen, R., Joshi, C., Kangasjärvi, J., Karlsson, J., Kelleher, C., Kirkpatrick, R., Kirst, M., Kohler, A., Kalluri, U., Larimer, F., Leebens-Mack, J., Leplé, J. C., Locascio, P., Lou, Y., Lucas, S., Martin, F., Montanini, B., Napoli, C., Nelson, D. R., Nelson, C., Nieminen, K., Nilsson, O., Pereda, V., Peter, G., Philippe, R., Pilate, G., Poliakov, A., Razumovskaya, J., Richardson, P., Rinaldi, C., Ritland, K., Rouzé, P., Ryaboy, D., Schmutz, J., Schrader, J., Segerman, B., Shin, H., Siddiqui, A., Sterky, F., Terry, A., Tsai, C. J., Uberbacher, E., Unneberg, P., Vahala, J., Wall, K., Wessler, S., Yang, G., Yin, T., Douglas, C., Marra, M., Sandberg, G., Van de Peer, Y., and Rokhsar, D. (2006). The genome of black cottonwood, *Populus trichocarpa* (Torr. & Gray). *Science* 313, 1596–1604.

Uggla, C., Mellerowicz, E., and Sundberg, B. (1998). Indole-3-acetic acid controls cambial growth in scots pine by positional signaling. *Plant Physiol.* 117, 113–121.

Uggla, C., Moritz, T., Sandberg, G., and Sundberg, B. (1996). Auxin as a positional signal in pattern formation in plants. *Proc. Natl. Acad. Sci. U.S.A.* 93, 9282–9286.

Utsuno, K., Shikanai, T., Yamada, Y., and Hashimoto, T. (1998). Agr, an Agravitropic locus of *Arabidopsis thaliana*, encodes a novel membrane-protein family member. *Plant Cell Physiol.* 39, 1111–1118.

Van Bel, A. J. E. (1990). Xylem-phloem exchange via the rays: the undervalued route of transport. *J. Exp. Bot.* 41, 631–644.

Vandesompele, J., De Preter, K., Pattyn, F., Poppe, B., Van Roy, N., De Paepe, A., and Speleman, F. (2002). Accurate normalization of real-time quantitative RT-PCR data by geometric averaging of multiple internal control genes. *Genome Biol.* 3, RESEARCH0034.

Varón, A., Vinh, L. S., and Wheeler, W. C. (2009). POY version 4: phylogenetic analysis using dynamic homologies. *Cladistics* 26, 72–85.

Vernoux, T., Brunoud, G., Farcot, E., Morin, V., Van den Daele, H., Legrand, J., Oliva, M., Das, P., Larrieu, A., Wells, D., Guédon, Y., Armitage, L., Picard, F., Guyomarc'h, S., Cellier, C., Parry, G., Koumproglou, R., Doonan, J. H., Estelle, M., Godin, C., Kepinski, S., Bennett, M., De Veylder, L., and Traas, J. (2011). The auxin signalling network translates dynamic input into robust patterning at the shoot apex. *Mol. Syst. Biol.* 7, 508.

Verrier, P. J., Bird, D., Burla, B., Dassa, E., Forestier, C., Geisler, M., Klein, M., Kolukisaoglu, U., Lee, Y., Martinoia, E., Murphy, A., Rea, P. A., Samuels, L., Schulz, B., Spalding, E. J., Yazaki, K., and Theodoulou, F. L. (2008). Plant ABC proteins – a unified nomenclature and updated inventory. *Trends Plant Sci.* 13, 151–159.

Vieten, A., Vanneste, S., Wisniewska, J., Benková, E., Benjamins, R., Beeckman, T., Luschnig, C., and Friml, J. (2005). Functional redundancy of PIN proteins is accompanied by auxin-dependent crossregulation of PIN expression. *Development* 132, 4521–4531.

Wang, J.-R., Hu, H., Wang, G.-H., Li, J., Chen, J.-Y., and Wu, P. (2009). Expression of PIN genes in rice (*Oryza sativa* L.): tissue specificity and regulation by hormones. *Mol. Plant* 2, 823–831.

Wheeler, W. (1996). Optimization alignment: the end of multiple sequence alignment in phylogenetics? *Cladistics* 12, 1–9.

Wiederstein, M., and Sippl, M. J. (2007). ProSA-web: interactive web service for the recognition of errors in three-dimensional structures of proteins. *Nucleic Acids Res.* 35, W407–W410.

Wolfe, K. H., Gouy, M., Yang, Y. W., Sharp, P. M., and Li, W. H. (1989). Date of the monocot-dicot divergence estimated from chloroplast DNA sequence data. *Proc. Natl. Acad. Sci. U.S.A.* 86, 6201–6205.

Wu, G., Lewis, D. R., and Spalding, E. P. (2007). Mutations in *Arabidopsis* multidrug resistance-like ABC transporters separate the roles of acropetal and basipetal auxin transport in lateral root development. *Plant Cell* 19, 1826–1837.

Wu, X., and McSteen, P. (2007). The role of auxin transport during inflorescence development in maize (*Zea mays*, Poaceae). *Am. J. Bot.* 94, 1745–1755.

Yang, H., and Murphy, A. S. (2009). Functional expression and characterization of *Arabidopsis* ABCB, AUX 1 and PIN auxin transporters in *Schizosaccharomyces pombe*. *Plant J.* 59, 179–191.

Yang, Y., Hammes, U. Z., Taylor, C. G., Schachtman, D. P., and Nielsen, E. (2006). High-affinity auxin transport by the AUX1 influx carrier protein. *Curr. Biol.* 16, 1123–1127.

Yemm, A., May, S., Williams, L., Millner, P., Tsurumi, S., Moore, I., Napier, R., Kerr, I. D., and Bennett, M. J. (2004). Structure-function analysis of the presumptive *Arabidopsis* auxin permease AUX1. *Plant Cell* 16, 3069–3083.

Zazímalová, E., Murphy, A. S., Yang, H., Hoyerová, K., and Hosek, P. (2010). Auxin transporters – why so many? *Cold Spring Harb. Perspect. Biol.* 2, 1–14.

APPENDIX

FIGURE A1 | Intron–exon structure of *PIN, AUX/LAX*, and *ABCB* genes from *Populus trichocarpa*.
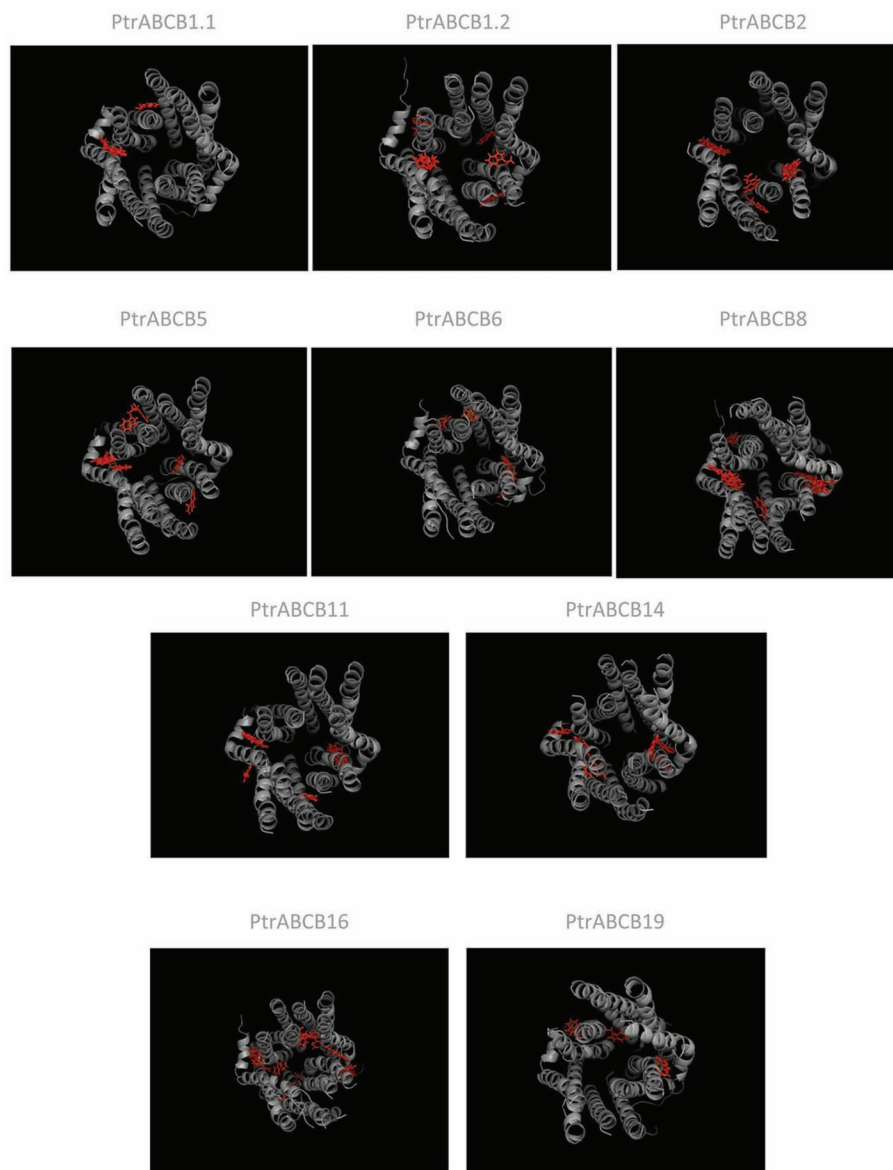
FIGURE A2 | Predicted model structures of putative auxin transport ABCBs from *Populus trichocarpa.* Tertiary protein structures have been generated using the python script Modeller 9v5. Predicted IAA docking sites are depicted in red.
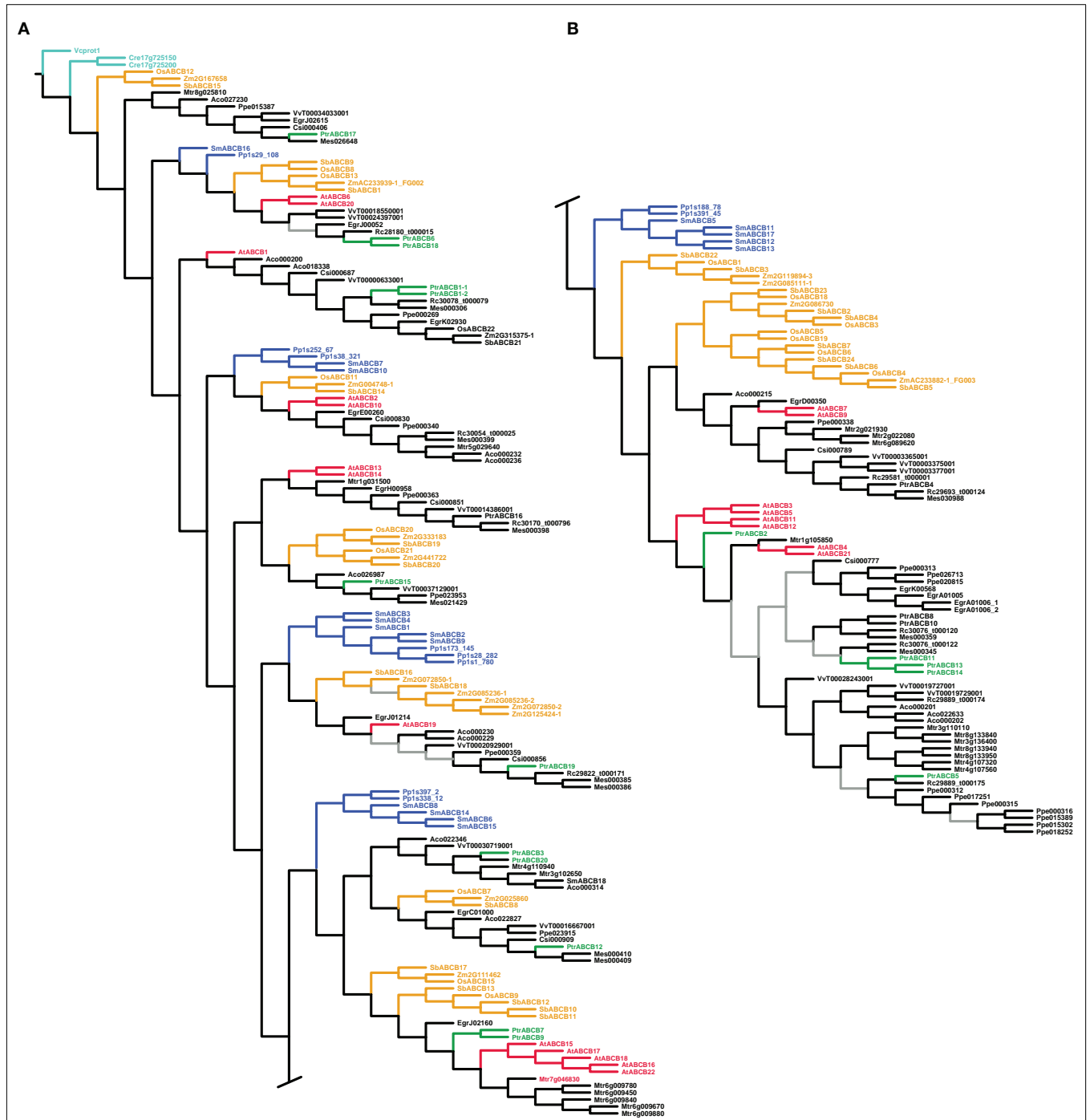
FIGURE A3 | Phylogeny of *ABCB* genes from land plants, based upon coding sequences from the loci listed in Table A4, analyzed using dynamic homology under the parsimony criterion. Gray branches indicate nodes with bootstrap support lower than 50%. Algal *ABCBs* are colored light blue–green, basal land plants blue, *Populus* green, *Arabidopsis* red, and monocots yellow. Abbreviated names of each species are listed in Table A1.

Table A1 | List of all species with their abbreviated names used in the present work.

Species	Abbreviation
Aquilegia caerulea	Aco
Arabidopsis thaliana	At
Chlamydomonas reinhardtii	Cre
Eucalyptus grandis	Egr
Manihot esculenta	Mes
Medicago truncatula	Mtr
Oryza sativa	Os
Physcomitrella patens	Pp
Populus tomentosa	Pto
Populus tremula × tremuloides	Ptt
Populus trichocarpa	Ptr
Prunus persica	Ppe
Ricinus communis	Rc
Selaginella moellendorffii	Sm
Sorghum bicolor	Sb
Vitis vinifera	Vv
Volvox carteri	Vc
Zea mays	Zm

Table A2 | List of putative auxin transport genes identified in the *Populus trichocarpa* genome.

Genes	JGI v1.1 gene model	JGI v1.1 locus
PtrPIN1	estExt_fgenesh4_pg.C_LG_XV0366	LG_XV:3955456–3958939
PtrPIN2	estExt_Genewise1_v1.C_LG_XVI1213	LG_XVI:2023747–2028247
PtrPIN3	gw1.X.6584.1	LG_X:11493441–11496545
PtrPIN4	estExt_fgenesh4_pm.C_LG_V0399	LG_V:12604974–12610191
PtrPIN5	fgenesh4_pm.C_LG_II000334	LG_II:4970467–4976705
PtrPIN6	fgenesh4_pm.C_LG_VIII000556	LG_VIII:8394273–8397294
PtrPIN7	estExt_Genewise1_v1.C_LG_XII1068	LG_XII:3820572–3824595
PtrPIN8	eugene3.00060333	LG_VI:2296469–2299715
PtrPIN9	fgenesh4_pm.C_LG_XVIII000434	LG_XVIII:12913539–12916356
PtrPIN10	fgenesh4_pm.C_LG_I000524	LG_I:12290101–12293363
PtrPIN11	estExt_fgenesh4_pg.C_870067	scaffold_87:1004073–1006598
PtrPIN12	fgenesh4_pg.C_LG_XIX000547	LG_XIX:6900262–6903432
PtrPIN13	fgenesh4_pg.C_LG_IV001142	LG_IV:12489496–12491318
PtrPIN14	gw1.XVII.929.1	LG_XVII:3836316–3838259
PtrPIN15	fgenesh4_pg.C_LG_XIV000875	LG_XIV:7307054–7309154
PtrPIN16	gw1.5147.2.1	scaffold_5147:1–1679
PtrAUX1/LAX5	grail3.0023028402	LG_VI:6769035–6772003
PtrAUX2/LAX1	eugene3.00161081	LG_XVI:10707443–10710997
PtrAUX3/LAX2	estExt_fgenesh4_pg.C_LG_X1704	LG_X:17003105–17007090
PtrAUX4/LAX6	estExt_Genewise1_v1.C_LG_VIII1679	LG_VIII:3795803–3800287
PtrAUX5/LAX7	estExt_fgenesh4_pg.C_LG_IV1437	LG_IV:15662320–15666183
PtrAUX6/LAX3	grail3.0001031001	LG_IX:2231536–2235747
PtrAUX7/LAX8	estExt_fgenesh4_pg.C_LG_V0933	LG_V:11098424–11101148
PtrAUX8/LAX4	grail3.0003074001	LG_II:6104679–6107343
PtrABCB1.1	gw1.28.733.1	scaffold_28:2297969–2304256
PtrABCB1.2	fgenesh4_pg.C_LG_XVI000833	LG_XVI:7805788–7812322
PtrABCB2	estExt_Genewise1_v1.C_LG_II3719	LG_II:16940658–16946357
PtrABCB3	eugene3.00130846	scaffold_1: 44776038–44781535
PtrABCB4	fgenesh4_pg.C_scaffold_204000026	scaffold_204:388201–394437
PtrABCB5	gw1.X.3657.1	LG_X:276730–282241
PtrABCB6	estExt_fgenesh4_pm.C_LG_X0835	LG_X:18271669–18278875
PtrABCB7	gw1.XVII.765.1	LG_XVII:3190614–3196509
PtrABCB8	estExt_fgenesh4_pm.C_LG_II0929	LG_II:16965413–16970969
PtrABCB9	fgenesh4_pg.C_LG_XVII000406	LG_XVII:4919010–4924173
PtrABCB10	eugene3.00140575	LG_XIV:4755266–4761017
PtrABCB11	eugene3.00140576	LG_XIV:4765985–4771483
PtrABCB12	gw1.XVIII.2596.1	LG_XVIII:8860516–8866795
PtrABCB13	eugene3.00140578	LG_XIV:4778008–4781195
PtrABCB14	estExt_fgenesh4_pm.C_LG_XIV0249	LG_XIV:4781910–4787506
PtrABCB15	fgenesh4_pm.C_LG_XV000001	LG_XV:12903–18128
PtrABCB16	fgenesh4_pm.C_LG_II000094	LG_II:1130589–1135712
PtrABCB17	eugene3.01580034	scaffold_158:318976–324742
PtrABCB18	fgenesh4_pg.C_LG_VIII000415	LG_VIII:2748354–2755879
PtrABCB19	estExt_fgenesh4_pg.C_LG_XVII0355	LG_XVII:4160851–4168120
PtrABCB20	fgenesh4_pm.C_LG_XI000351	scaffold_11:16,395,988.0.16,402,087

(Continued)

Table A2 | Continued

Genes	Phytozome v.7.0 locus	GenBank accesion number	Chrom.	Closest similar sequence
PtrPIN1	POPTR_0015s04570	XM_002322068	chr.15	PtrPIN7
PtrPIN2	POPTR_0016s03450	XM_002322578	chr.16	PtrPIN8
PtrPIN3	POPTR_0010s12320	XM_002314774	chr.10	PtrPIN6
PtrPIN4	POPTR_0005s20990	XM_002306642	chr.5	PtrPIN5
PtrPIN5	POPTR_0002s07310	XM_002302160	chr.2	PtrPIN4
PtrPIN6	POPTR_0008s12830	XM_002312400	chr.8	PtrPIN3
PtrPIN7	POPTR_0012s04470	XM_002317838	chr.12	PtrPIN1
PtrPIN8	POPTR_0006s03540	XM_002307930	chr.6	PtrPIN2
PtrPIN9	POPTR_0018s13610	XM_002324641	chr.18	No clear match
PtrPIN10	POPTR_0001s21230	XM_002298168	chr.1	No clear match
PtrPIN11	POPTR_0013s08510	XM_002328968	chr.13	PtrPIN12
PtrPIN12	POPTR_0019s07990	XM_002325430	chr.19	PtrPIN11
PtrPIN13	POPTR_0004s12310	XM_002305335	chr.4	PtrPIN14
PtrPIN14	POPTR_0017s11440	NC_008483	chr.17	PtrPIN13
PtrPIN15	POPTR_0014s14390[a]	XM_002320399	chr.14	No clear match
PtrPIN16	POPTR_0014s14390[a]	XM_002336619	chr.2	No clear match
PtrAUX1/LAX5	POPTR_0006s09940	XM_002309092	chr.6	PtrAUX2/LAX1
PtrAUX2/LAX1	POPTR_0016s12100	XM_002322933	chr.16	PtrAUX1/LAX5
PtrAUX3/LAX2	POPTR_0010s19840	XM_002316190	chr.10	PtrAUX4/LAX6
PtrAUX4/LAX6	POPTR_0008s06630	XM_002311172	chr.8	PtrAUX3/LAX2
PtrAUX5/LAX7	POPTR_0004s17860	XM_002306139	chr.4	PtrAUX6/LAX3
PtrAUX6/LAX3	POPTR_0009s13470	XM_002312937	chr.9	PtrAUX5/LAX7
PtrAUX7/LAX8	POPTR_0005s16020	XM_002306579	chr.5	PtrAUX8/LAX4
PtrAUX8/LAX4	POPTR_0002s08750	XM_002302217	chr.2	PtrAUX7/LAX8
PtrABCB1.1	POPTR_0006s12590	XM_002323449	chr.6	PtrABCB1.2
PtrABCB1.2	POPTR_0016s09680	XM_002519442	chr.16	PtrABCB1.1
PtrABCB2	POPTR_0002s18860	XM_002301511	chr.2	PtrABCB10
				PtrABCB11
				PtrABCB13
				PtrABCB14
PtrABCB3	POPTR_0001s44320	XM_002319243	chr.1	PtrABCB20
PtrABCB4	POPTR_0001s34280	XM_002331841	chr.1	No clear match
PtrABCB5	POPTR_0010s00540	XM_002314297	chr.10	No clear match
PtrABCB6	POPTR_0010s21720	XM_002316273	chr.10	PtrABCB18
PtrABCB7	POPTR_0017s11030	XM_002323983	chr.17	No clear match
PtrABCB8	POPTR_0002s18850	XM_002301514	chr.2	PtrABCB10
				PtrABCB11
PtrABCB9	POPTR_0017s12120	XM_002323830	chr.17	POPTR_0004s12180
PtrABCB10	POPTR_0014s10860	XM_002320902	chr.14	PtrABCB2, PtrABCB8
PtrABCB11	POPTR_0014s10870	XM_002320903	chr.14	PtrABCB2, PtrABCB8
PtrABCB12	POPTR_0018s09420	XM_002324987	chr.18	No clear match
PtrABCB13	POPTR_0014s10880.1	XM_002320905	chr.14	PtrABCB2, PtrABCB8
PtrABCB14	POPTR_0014s10880.2	XM_002320906	chr.14	PtrABCB2, PtrABCB8
PtrABCB15	POPTR_0015s00250	XM_002321303	chr.15	POPTR_0012s00290[c]
				POPTR_0012s00360[b]
				POPTR_0012s00370[c]

(Continued)

Table A2 | Continued

Genes	Phytozome v.7.0 locus	GenBank accesion number	Chrom.	Closest similar sequence
PtrABCB16	POPTR_0002s02110	XM_002301925	chr.2	No clear match
PtrABCB17	POPTR_0001s16560	XM_002331169	chr.1	No clear match
PtrABCB18	POPTR_0008s05020	XM_002311108	chr.8	PtrABCB6
PtrABCB19	POPTR_0017s11750	XM_002323811	chr.17	No clear match
PtrABCB20	POPTR_0011s13720	XM_002316941	chr.11	PtrABCB3

Gene models, accession numbers, chromosome position, and the closest most similar match for each gene are reported.

[a]These genes are distinct in GenBank but they retrieve the same entry in the phytozome database (www.phytozome.org).

[b]Very short protein classified as ATP-binding transporter.

[c]Uncharacterized conserved protein.

Table A3 | Summary of the protein characteristics of the PIN, AUX/LAX, and ABCB families of *Populus trichocarpa,* *Populus tomentosa,* *Populus* *tremula* × *tremuloides,* **and** *Arabidopsis.*

Gene	length cds (bp)	Length Protein (aa)	*n* TMHs	Type
AtPIN1	1869	622	11	Long
AtPIN2	1944	647	10	Long
AtPIN3	1923	640	10	Long
AtPIN4	1851	616	10	Long
AtPIN5	1056	351	10	Short
AtPIN6	1713	570	10	Reduced
AtPIN7	1860	619	10	Long
AtPIN8	1104	367	10	Short
PtrPIN1	1845	614	10	Long
PtrPIN2	1767	588	11	Long
PtrPIN3	1905	634	10	Long
PtrPIN4	1338	446	9	Reduced
PtrPIN5	1110	369	8	Reduced
PtrPIN6	1950	650	10	Long
PtrPIN7	1830	610	10	Long
PtrPIN8	1764	588	10	Long
PtrPIN9	1902	634	10	Long
PtrPIN10	1644	548	10	Reduced
PtrPIN11	1041	347	9	Short
PtrPIN12	1041	347	10	Short
PtrPIN13	1068	356	8	Short
PtrPIN14	1071	357	8	Short
PtrPIN15	1113	371	8	Short
PtrPIN16	912	304	6	Short
PttPIN1	1845	614	10	Long
PttPIN2	1767	588	10	Long
PttPIN3	1923	640	10	Long
PtoPIN1	1860	619	9	Long
AtAUX1	1458	485	11	
AtLAX1	1467	489	11	
AtLAX2	1452	484	11	
AtLAX3	1413	471	11	
PtrAUX1/LAX5	1443	481	11	
PtrAUX2/LAX1	1434	478	11	
PtrAUX3/LAX2	1422	474	11	
PtrAUX4/LAX6	1416	472	11	
PtrAUX5/LAX7	1476	492	11	
PtrAUX6/LAX3	1476	492	11	
PtrAUX7/LAX8	1395	465	11	
PtrAUX8/LAX4	1398	466	11	
PttLAX1	1434	477	10	
PttLAX2	1422	473	11	
PttLAX3	1476	491	11	
PtoAUX1	1434	477	10	
AtABCB1	3861	1286	12	
AtABCB2	3822	1273	12	
AtABCB3	3690	1229	11	
AtABCB4	3861	1286	9	
AtABCB5	3693	1230	9	
AtABCB6	4224	1407	13	

(Continued)

Table A3 | Continued

Gene	Length cds (bp)	Length Protein (aa)	*n* TMHs
AtABCB7	3747	1248	11
AtABCB8	3723	1241	12
AtABCB9	3711	1236	9
AtABCB10	3684	1227	10
AtABCB11	3837	1278	9
AtABCB12	3822	1273	9
AtABCB13	3738	1245	11
AtABCB14	3744	1247	11
AtABCB15	3723	1240	11
AtABCB16	3687	1228	7
AtABCB17	3723	1240	9
AtABCB18	3678	1225	9
AtABCB19	3759	1252	10
AtABCB20	4227	1408	13
AtABCB21	3891	1296	9
AtABCB22	3666	1221	7
PtrABCB1.1	4074	1357	12
PtrABCB1.2	3975	1324	12
PtrABCB2	3687	1228	10
PtrABCB3	3756	1251	9
PtrABCB4	3768	1255	10
PtrABCB5	3882	1294	9
PtrABCB6	4194	1398	12
PtrABCB7	3780	1260	11
PtrABCB8	3828	1276	11
PtrABCB9	3717	1239	9
PtrABCB10	3864	1287	9
PtrABCB11	3882	1294	9
PtrABCB12	3693	1230	8
PtrABCB13	3597	1199	7
PtrABCB14	3885	1294	9
PtrABCB15	3828	1276	10
PtrABCB16	3660	1220	11
PtrABCB17	4644	1548	12
PtrABCB18	4197	1399	12
PtrABCB19	3756	1252	10
PtrABCB20	3516	1171	10

All proteins are classified according to their sequence length, number of predicted transmembrane helices, and length of the central hydrophilic loop (short, reduced, long).

Table A4 | List of all the sequences used in the reconstruction of *PIN, AUX/LAX,* and *ABCB* families phylogenies.

Phytozome database locus or GenBank accession number	Assigned name
ABCBs	
ppa000359m.g	Ppe000359
ppa000340m.g	Ppe000340
ppa000269m.g	Ppe000269
ppa000313m.g	Ppe000313
ppa000316m.g	Ppe000316
ppa023953m.g	Ppe023953
ppa000315m.g	Ppe000315
ppa015302m.g	Ppe015302
ppa000363m.g	Ppe000363
ppa015387m.g	Ppe015387
ppa015389m.g	Ppe015389
ppa017251m.g	Ppe017251
ppa023915m.g	Ppe023915
ppa018252m.g	Ppe018252
ppa000312m.g	Ppe000312
ppa026713m.g	Ppe026713
ppa000338m.g	Ppe000338
ppa0208157m.g	Ppe020815
POPTR_0006s12590	PtrABCB11
POPTR_0016s09680	PtrABCB12
POPTR_0002s18860	PtrABCB2
POPTR_0001s44320	PtrABCB3
POPTR_0001s34280	PtrABCB4
POPTR_0010s00540	PtrABCB5
POPTR_0010s21720	PtrABCB6
POPTR_0017s11030	PtrABCB7
POPTR_0002s18850	PtrABCB8
POPTR_0017s12120	PtrABCB9
POPTR_0014s10860	PtrABCB10
POPTR_0014s10870	PtrABCB11
POPTR_0018s09420	PtrABCB12
POPTR_0014s10880.1	PtrABCB13
POPTR_0014s10880.2	PtrABCB14
POPTR_0015s00250	PtrABCB15
POPTR_0002s02110	PtrABCB16
POPTR_0001s16560	PtrABCB17
POPTR_0008s05020	PtrABCB18
POPTR_0017s11750	PtrABCB19
POPTR_0011s13720	PtrABCB20
GRMZM2G315375_T01	Zm2G315375-1
GRMZM2G085236_T01	Zm2G085236-1
GRMZM2G085236_T02	ZmG085236-2
GRMZM2G004748_T01	ZmG004748-1
GRMZM2G119894_T01	Zm2G119894-1
GRMZM2G119894_T03	Zm2G119894-3
GRMZM2G086730_T01	Zm2G086730
AC233882.1_FGT003	ZmAC233882-1_FG003
GRMZM2G025860_T01	Zm2G025860
GRMZM2G167658_T01	Zm2G167658
GRMZM2G111462_T01	Zm2G111462
GRMZM2G085111_T02	Zm2G085111-1

(Continued)

Table A4 | Continued

Phytozome database locus or GenBank accession number	Assigned name
GRMZM2G333183_T01	Zm2G333183
AC233939.1_FGT002	ZmAC233939-1_FG002
GRMZM2G441722_T01	Zm2G441722
Eucrg.J2160.1	EgrJ02160
Eucgr.D00350.1	EgrD00350
Eucgr.K00568.1	EgrK00568-1
Eucgr.K02930.1	EgrK02930
Eucgr.E00260.1	EgrE00260
Eucgr.C01000.1	EgrC01000
Eucgr.A01005.1	EgrA01005
Eucgr.A01006.1	EgrA01006-1
Eucgr.A01006.2	EgrA01006-2
Eucgr.J01214.1	EgrJ01214
Eucgr.J02615.1	EgrJ02615
Eucgr.H00958.1	EgrH00958
Eucgr.J00052.1	EgrJ00052
cassava4.1_000398m.g	Mes000398
cassava4.1_000345m.g	Mes000345
cassava4.1_000359m.g	Mes000359
cassava4.1_030988m.g	Mes030988
cassava4.1_000410m.g	Mes000410
cassava4.1_000306m.g	Mes000306
cassava4.1_000385m.g	Mes000385
cassava4.1_000386m.g	Mes000386
cassava4.1_000399m.g	Mes000399
cassava4.1_000409m.g	Mes000409
cassava4.1_026648m.g	Mes026648
cassava4.1_021429m.g	Mes021429
Medtr5g029640.1	Mtr5g029640
Medtr1g031500.1	Mtr1g031500
Medtr2g022080.1	Mtr2g022080
Medtr6g089620.1	Mtr6g089620
Medtr2g021930.1	Mtr2g021930
Medtr1g105850.1	Mtr1g105850
Medtr8g078020.1	Mtr8g078020
Medtr6g009670.1	Mtr6g009670
Medtr8g133940.1	Mtr8g133940
Medtr3g110110.1	Mtr3g110110
Medtr8g133950.1	Mtr8g133950
Medtr8g133840.1	Mtr8g133840
Medtr4g107320.1	Mtr4g107320
Medtr4g107560.1	Mtr4g107560
Medtr6g009780.1	Mtr6g009780
Medtr6g009880.1	Mtr6g009880
Medtr6g009840.1	Mtr6g009840
Medtr3g136400.1	Mtr3g136400
Medtr7g046830.1	Mtr7g046830
Medtr6g009450.1	Mtr6g009450
Medtr3g102650.1	Mtr3g102650
Medtr8g025810.1	Mtr8g025810
Medtr4g110940.1	Mtr4g110940
GSVIVT00000633001	VvT00000633001

(Continued)

Table A4 | Continued

Phytozome database locus or GenBank accession number	Assigned name
GSVIVT00003365001	VvT00003365001
GSVIVT00003375001	VvT00003375001
GSVIVT00003377001	VvT00003377001
GSVIVT00014386001	VvT00014386001
GSVIVT00016667001	VvT00016667001
GSVIVT00018550001	VvT00018550001
GSVIVT00019727001	VvT00019727001
GSVIVT00019729001	VvT00019729001
GSVIVT00020929001	VvT00020929001
GSVIVT00024397001	VvT00024397001
GSVIVT00028243001	VvT00028243001
GSVIVT00030719001	VvT00030719001
GSVIVT00034033001	VvT00034033001
GSVIVT00037129001	VvT00037129001
Sb01g039110.1	SbABCB1
Sb02g019540.1	SbABCB2
Sb03g011860.1	SbABCB3
Sb03g023740.1	SbABCB4
Sb03g031990.1	SbABCB5
Sb03g032000.1	SbABCB6
Sb03g032030.1	SbABCB7
Sb03g033290.1	SbABCB8
Sb03g047490.1	SbABCB9
Sb04g006087.1	SbABCB10
Sb04g006090.1	SbABCB11
Sb04g006100.1	SbABCB12
Sb04g022480.1	SbABCB13
Sb04g031170.1	SbABCB14
Sb06g001440.1	SbABCB15
Sb06g018860.1	SbABCB16
Sb06g020350.1	SbABCB17
Sb06g030350.1	SbABCB18
Sb07g003510.1	SbABCB19
Sb07g003520.1	SbABCB20
Sb07g023730.1	SbABCB21
Sb09g002940.1	SbABCB22
Sb09g027320.1	SbABCB23
Sb09g027330.1	SbABCB24
e_gw1.13.597.1	SmABCB1
fgenesh1_pm.C_scaffold_6000062	SmABCB2
fgenesh2_pg.C_scaffold_13000013	SmABCB3
e_gw1.6.146.1	SmABCB4
estExt_Genewise1Plus.C_350372	SmABCB5
fgenesh1_pm.C_scaffold_42000045	SmABCB6
e_gw1.0.369.1	SmABCB7
fgenesh2_pg.C_scaffold_9000128	SmABCB8
estExt_Genewise1.C_210058	SmABCB9
fgenesh1_pm.C_scaffold_2000054	SmABCB10
e_gw1.73.37.1	SmABCB11
estExt_Genewise1Plus.C_90010	SmABCB12
e_gw1.0.1863.1	SmABCB13
e_gw1.22.307.1	SmABCB14

(Continued)

Table A4 | Continued

Phytozome database locus or GenBank accession number	Assigned name
fgenesh1_pm.C_scaffold_0000169	SmABCB15
estExt_Genewise1.C_00569	SmABCB16
e_gw1.73.196.1	SmABCB17
fgenesh1_pm.C_scaffold_15000068	SmABCB18
LOC_Os01g18670.1	OsABCB1
LOC_Os01g35030.1	OsABCB3
LOC_Os01g50080.1	OsABCB4
LOC_Os01g50100.1	OsABCB5
LOC_Os01g50160.1	OsABCB6
LOC_Os01g52550.1	OsABCB7
LOC_Os01g74470.1	OsABCB8
LOC_Os02g09720.1	OsABCB9
LOC_Os02g46680.1	OsABCB11
LOC_Os03g08380.1	OsABCB12
LOC_Os03g17180.1	OsABCB13
LOC_Os04g40570.1	OsABCB15
LOC_Os05g47490.1	OsABCB18
LOC_Os05g47500.1	OsABCB19
LOC_Os08g05690.1	OsABCB20
LOC_Os08g05710.1	OsABCB21
LOC_Os08g45030.1	OsABCB22
Rco30078.t000079	Rc30078_t000079
Rco30054.t000025	Rc30054_t000025
Rco30076.t000120	Rc30076_t000120
Rco30076.t000122	Rc30076_t000122
Rco28180.t000015	Rc28180_t000015
Rco30170.t000796	Rc30170_t000796
Rco29581.t000001	Rc29581_t000001
Rco29693.t000124	Rc29693_t000124
Rco29822.t000171	Rc29822_t000171
Rco29889.t000174	Rc29889_t000174
Rco29889.t000175	Rc29889_t000175
Pp1s252_67V6.1	Pp1s252_67
Pp1s38_321V6.1	Pp1s38_321
Pp1s28_282V6.1	Pp1s28_282
Pp1s173_145V6.1	Pp1s173_145
Pp1s1_780V2.1	Pp1s1_780
Pp1s397_2V6.1	Pp1s397_2
Pp1s188_78V6.1	Pp1s188_78
Pp1s391_45V6.1	Pp1s391_45
Pp1s338_12V6.1	Pp1s338_12
Pp1s29_108V2.1	Pp1s29_108
Vc_estExt_fgenesh4_pg.C_30286	VcProt1
Cre17.g725200	Cre17_g725200
Cre17.g725150	Cre17_g725150
AT2G36910	AtABCB1
AT4G25960	AtABCB2
AT4G01820	AtABCB3
AT2G47000	AtABCB4
AT4G01830	AtABCB5
AT2G39480	AtABCB6
AT5G46540	AtABCB7

(Continued)

Table A4 | Continued

Phytozome database locus or GenBank accession number	Assigned name
AT3G30875	AtABCB8
AT4G18050	AtABCB9
AT1G10680	AtABCB10
At1g02520	AtABCB11
AT1G02530	AtABCB12
AT1G27940	AtABCB13
AT1G28010	AtABCB14
AT3G28345	AtABCB15
AT3G28360	AtABCB16
AT3G28380	AtABCB17
AT3G28390	AtABCB18
AT3G28860	AtABCB19
AT3G55320	AtABCB20
AT3G62150	AtABCB21
AT3G28415	AtABCB22
orange1.1g000851m.g	Csi_g000851
orange1.1g000777m.g	Csi_g000777
orange1.1g000789m.g	Csi_g000789
orange1.1g000909m.g	Csi_g000909
orange1.1g000830m.g	Csi_g000830
orange1.1g000406m.g	Csi_g000406
orange1.1g000687m.g	Csi_g000687
orange1.1g000856m.g	Csi_g000856
AcoGoldSmith_v1.000232m.g	Aco000232
AcoGoldSmith_v1.022827m.g	Aco022827
AcoGoldSmith_v1.027230m.g	Aco027230
AcoGoldSmith_v1.000200m.g	Aco000200
AcoGoldSmith_v1.018338m.g	Aco018338
AcoGoldSmith_v1.000314m.g	Aco000314
AcoGoldSmith_v1.022346m.g	Aco022346
AcoGoldSmith_v1.026987m.g	Aco026987
AcoGoldSmith_v1.022633m.g	Aco022633
AcoGoldSmith_v1.000202m.g	Aco000202
AcoGoldSmith_v1.000201m.g	Aco000201
AcoGoldSmith_v1.000230m.g	Aco000230
AcoGoldSmith_v1.000215m.g	Aco000215
AcoGoldSmith_v1.000236m.g	Aco000236
AcoGoldSmith_v1.000229m.g	Aco000229
AUX/LAXs	
ppa005323m.g	Ppe005323
ppa005057m.g	Ppe005057
ppa004949m.g	Ppe004949
ppa004865m.g	Ppe004865
POPTR_0006s09940	PtrAUX1/LAX5
POPTR_0016s12100	PtrAUX2/LAX1
POPTR_0010s19840	PtrAUX3/LAX2
POPTR_0008s06630	PtrAUX4/LAX6
POPTR_0004s17860	PtrAUX5/LAX7
POPTR_0009s13470	PtrAUX6/LAX3
POPTR_0005s16020	PtrAUX7/LAX8
POPTR_0002s08750	PtrAUX8/LAX4
GRMZM2G067022_T01	Zm2G067022

(Continued)

Table A4 | Continued

Phytozome database locus or GenBank accession number	Assigned name
GRMZM2G127949_T01	Zm2G127949
GRMZM2G045057_T01	Zm2G045057
GRMZM2G149481_T01	Zm2G149481
GRMZM2G129413_T01	Zm2G129413
Eucgr.F03758.1	EgrF03758_1
Eucgr.K02992.2	EgrK02992_2
Eucgr.G03044.2	EgrG03044_2
Eucgr.G01769.2	EgrG01769_2
Eucgr.A00514.2	EgrA00514_2
cassava4.1_006838m.g	Mes006838
cassava4.1_006423m.g	Mes006423
cassava4.1_006788m.g	Mes006788
cassava4.1_006570m.g	Mes006570
cassava4.1_006783m.g	Mes006783
cassava4.1_006474m.g	Mes006474
cassava4.1_007093m.g	Mes007093
Medtr3g024670.1	Mtr3g024670
Medtr3g097960.1	Mtr3g097960
Medtr5g089600.1	Mtr5g089600
GSVIVT01008917001	VvT01008917001
GSVIVT01024054001	VvT01024054001
GSVIVT01032855001	VvT01032855001
GSVIVT01033986001	VvT01033986001
Sb01g026240.1	SbLAX1
Sb01g041270.1	SbLAX2
Sb03g040320.1	SbLAX3
Sb05g004250.1	SbLAX4
Sb09g021990.1	SbLAX5
estExt_Genewise1Plus.C_20968	SmAUX1
estExt_fgenesh2_pg.C_50586	SmAUX2
LOC_Os01g63770.1	OsLAX1
LOC_Os03g14080.1	OsLAX2
LOC_Os05g37470.1	OsLAX3
LOC_Os10g05690.1	OsLAX4
LOC_Os11g06820.1	OsLAX5
Rco29669.t000030	Rc29669_t000030
Rco29741.t000002	Rc29741_t000002
Rco29908.t000197	Rc29908_t000197
Rco29969.t000004	Rc29969_t000004
Pp1s90_46V6.1	Pp1s90_46
Pp1s213_89V6.1	Pp1s213_89
Pp1s211_67V6.1	Pp1s211_67
AT2G38120.1	AtAUX1
AT5G01240.1	AtLAX1
AT2G21050.1	AtLAX2
AT1G77690.1	AtLAX3
orange1.1g011392m.g	Csi_g011392
orange1.1g011022m.g	Csi_g011022
orange1.1g012371m.g	Csi_g012371
orange1.1g011966m.g	Csi_g011966
AcoGoldSmith_v1.004219m.g	Aco004219
AcoGoldSmith_v1.004342m.g	Aco004342

(Continued)

Table A4 | Continued

Phytozome database locus or GenBank accession number	Assigned name
AcoGoldSmith_v1.003895m.g	Aco003895
AY864733	Pto-AY864733
AF115543	Ptt-AF115543
PINs	
ppa022797m.g	Ppe022797
ppa003159m.g	Ppe003159
ppa024134m.g	Ppe024134
ppa002528m.g	Ppe002528
ppa025174m.g	Ppe025174
ppa002944m.g	Ppe002944
ppa021573m.g	Ppe021573
ppa007621m.g	Ppe007621
POPTR_0015s04570	PtrPIN1
POPTR_0016s03450	PtrPIN2
POPTR_0010s12320	PtrPIN3
POPTR_0005s20990	PtrPIN4
POPTR_0002s07310	PtrPIN5
POPTR_0008s12830	PtrPIN6
POPTR_0012s04470	PtrPIN7
POPTR_0006s03540	PtrPIN8
POPTR_0018s13610	PtrPIN9
POPTR_0001s21230	PtrPIN10
POPTR_0013s08510	PtrPIN11
POPTR_0019s07990	PtrPIN12
POPTR_0004s12310	PtrPIN13
POPTR_0017s11440	PtrPIN14
POPTR_0014s14390	PtrPIN15
XM_002336619.1	PtrPIN16
ZmPIN1a_GRMZM2G098643	ZmPIN1a
ZmPIN1b_GRMZM2G074267	ZmPIN1b
ZmPIN1c_GRMZM2G149184	ZmPIN1c
ZmPIN1d_GRMZM2G171702_T01	ZmPIN1d
ZmPIN2	ZmPIN2
ZmPIN5a-GRMZM2G025742	ZmPIN5a
ZmPIN5b-GRMZM2G148648	ZmPIN5b
ZmPIN5c-GRMZM2G040911	ZmPIN5c
ZmPIN8_GRMZM5G839411	ZmPIN8
ZmPIN9_GRMZM5G859099	ZmPIN9
ZmPIN10a-GRMZM2G126260	ZmPIN10a
ZmPIN10b-GRMZM2G160496	ZmPIN10b
Eucgr.F04265.1	EgrF04265_1
Eucgr.K02271.1	EgrK02271_1
Eucgr.G02187.1	EgrG02187_1
Eucgr.G02549.1	EgrG02549_1
Eucgr.B01406.1	EgrB01406_1
Eucgr.B02902.1	EgrB02902_1
Eucgr.B00948.1	EgrB00948_1
Eucgr.C00078.1	EgrC00078_1
Eucgr.A02229.1	EgrA02229_1
Eucgr.H01390.1	EgrH01390_1
Eucgr.H01391.1	EgrH01391_1
Eucgr.I01919.1	EgrI01919_1

(Continued)

Table A4 | Continued

Phytozome database locus or GenBank accession number	Assigned name
Eucgr.G02548.1	EgrG02548_1
Eucgr.B01405.1	EgrB01405_1
Eucgr.B01403.1	EgRB01403_1
Eucgr.H01382.1	EgrH01382_1
cassava4.1_003807m.g	Mes003807
cassava4.1_030090m.g	Mes030090
cassava4.1_029078m.g	Mes029078
cassava4.1_003367m.g	Mes003367
cassava4.1_006998m.g	Mes006998
cassava4.1_026579m.g	Mes026579
cassava4.1_003794m.g	Mes003794
cassava4.1_029063m.g	Mes029063
cassava4.1_033391m.g	Mes033391
cassava4.1_010688m.g	Mes010688
cassava4.1_010607m.g	Mes010607
Medtr2g043210	Mtr2g043210
Medtr4g154810	Mtr4g154810
Medtr6g083450	Mtr6g083450
Medtr7g008720	Mtr7g008720
Medtr7g089430	Mtr7g089430
Medtr7g106430	Mtr7g106430
Medtr8g130020	Mtr8g130020
Medtr8g130040	Mtr8g130040
MtrAAM55297	MtrAAM55297
MtrAY115838	MtrAY115838
MtrAAT48627	MtrAAT48627
GSVIVT00014302001	VvT00014302001
GSVIVT00017824001	VvT00017824001
GSVIVT00020886001	VvT00020886001
GSVIVT00023254001	VvT00023254001
GSVIVT00023255001	VvT00023255001
GSVIVT00025093001	VvT00025093001
GSVIVT00025108001	VvT00025108001
GSVIVT00030482001	VvT00030482001
GSVIVT00031315001	VvT00031315001
Sb02g029210.1	SbPIN1
Sb03g029320.1	SbPIN2
Sb03g032850.1	SbPIN3
Sb03g037350.1	SbPIN4
Sb03g043960.1	SbPIN5
Sb04g028170.1	SbPIN6
Sb05g002150.1	SbPIN7
Sb07g026370.1	SbPIN8
Sb10g004430.1	SbPIN9
Sb10g008290.1	SbPIN10
Sb10g026300.1	SbPIN11
e_gw1.26.13.1	Sm102666
e_gw1.59.169.1	Sm119024
fgenesh1_pm.C_scaffold_9000007	Sm231064
fgenesh1_pm.C_scaffold_59000022	Sm234325
estExt_fgenesh1_pm.C_500006	Sm268490

(Continued)

Table A4 | Continued

Phytozome database locus or GenBank accession number	Assigned name
e_gw1.21.81.1	Sm99301
Os01g45550.1	OsPIN10a
Os01g51780	OsPIN8
Os01g58860	OsPIN9
Os01g69070	OsPIN5a
Os02g50960.1	OsPIN1b
Os05g50140	OsPIN10b
Os06g12610	OsPIN1a
Os06g44970	OsPIN2
Os08g41720	OsPIN5b
Os09g32770	OsPIN5c
Os11g04190	OsPIN1c
Os12g04000	OsPIN1d
Rco27985.t000045	Rc27985_t000045
Rco29662.t000026	Rc29662_t000026
Rco29816.t000014	Rc29816_t000014
Rco30180.t000054	Rc30180_t000054
Rco29822.t000149	Rc29822_t000149
Rco30128.t000486	Rc30128_t000486
Pp1s10_17V6.1	PpPIN1A
Pp1s18_186V6.1	PpPIN1B
Pp1s32_43V6.1	PpPIN1C
Pp1s79_126V6	PpPIN1D
AT1G73590	AtPIN1
AT5G57090	AtPIN2
AT1G70940	AtPIN3
AT2G01420	AtPIN4
AT5G16530	AtPIN5
AT1G77110	AtPIN6
AT1G23080	AtPIN7
AT5G15100	AtPIN8
orange1.1g006199m.g	Csi_g006199
orange1.1g007826m.g	Csi_g007826
orange1.1g036474m.g	Csi_g036474
orange1.1g041301m.g	Csi_g041301
orange1.1g048649m.g	Csi_g048649
orange1.1g035534m.g	Csi_g035534
orange1.1g007420m.g	Csi_g007420
orange1.1g018360m.g	Csi_g018360
orange1.1g019021m.g	Csi_g019021
AcoGoldSmith_v1.001931m.g	Aco001931
AcoGoldSmith_v1.018694m.g	Aco018694
AcoGoldSmith_v1.018139m.g	Aco018139
AcoGoldSmith_v1.016169m.g	Aco016169
AcoGoldSmith_v1.007499m.g	Aco007499
AcoGoldSmith_v1.021242m.g	Aco021242
AY302060	PtoPIN1-like
AF190881	PttPIN1
AF515435	PttPIN2
AF515434	PttPIN3

Table A5 | List of all primers used in the present work.

Name	Direction	Sequence (5′–3′)	Tm (°C)[a]	Amplicon (bp)
PIN1 RT-F3	Forward	AAGCTGAAGATGGTAGGGACCTT	58	94
PIN1 RT-R3	Reverse	TGGGCGCCATAATCATGAC	59	
PIN2 RT-F4	Forward	GATCAATGTTCAGGGATCAACAGA	59	81
PIN2 RT-R4	Reverse	GTTGTTGGTGGAAATGAAGTGAAA	59	
PIN3 RT-F3	Forward	CTTCACGTTGCTATTGTTCAGG	54.1	238
PIN3 RT-R3	Reverse	TGACACACGACCAGCAAGTAA	56.5	
PIN4 RT-F4	Forward	CGTTGGAATGAGAGGAGTGC	55	204
PIN4 RT-R4	Reverse	AATCTAAATTCCCCCTCTAATTCATGG	54.8	
PIN5 RT-F2	Forward	GACTAATGCAACCAACACACCTTT	58	67
PIN5 RT-R2	Reverse	TGGATGCCGGGATATTTTACC	59	
PIN6 RT-F2	Forward	CCATTCCACAAGCTGGAAATT	53.7	166
PIN6 RT-R2	Reverse	CCGGAATCTGGAGCGCCGA	62.6	
PIN7 RT-F4	Forward	TCAGTGCTCGGGCATCAA	58	81
PIN7 RT-R4	Reverse	GGATCATTAGTAGATATGAAGTGGAAAGAG	58	
PIN8 RT-F2	Forward	CTTCATTTGCTGTTGGACTACG	54.1	192
PIN8 RT-R2	Reverse	GTCCAAGCAAAATATAGTAAACCAGTGT	55.6	
PIN9 RT-F2	Forward	GCTGCTTTTCAACCTGAATCCG	57	173
PIN9 RT-R2	Reverse	TCTGCTGCCATATCCATCTTCTTTTG	57.3	
PIN10 RT-F4	Forward	GGCAGACACACCTACCCTGATC	59.4	100
PIN10 RT-R4	Reverse	CCGGAGGCATCTGTTGTTTC	56.3	
PIN11 RT-F3	Forward	CAGCATTGCCACAGTCAATTACATC	56.8	196
PIN11 RT-R3	Reverse	GCCGAGCTATATTCCTCCTTCAAG	57	
PIN12 RT-F6	Forward	GCTACGGCTGGTCCATTACC	58	100
PIN12 RT-R6	Reverse	ACTGCCGTCGGCCCATA	59.6	
PIN13 RT-F2	Forward	GGATACATTGAGCACAGGGGTAA	56.6	199
PIN13 RT-R2	Reverse	TGGACGGGACAGACTTCTATGATTC	57.9	
PIN14 RT-F3	Forward	ATAGTGATATTGTCAACAGGAGGG	54.1	175
PIN14 RT-R3	Reverse	CCAGTCTAACGGCGAAGGAAG	57.6	
PIN15 RT-F2	Forward	TTTGCTGGGCTAATTTCTCAAGA	55.5	188
PIN15 RT-R1	Reverse	AGTGGGATCCCCATCACAAG	54.9	
PIN16 RT-F4	Forward	GGTAACAATCTTGTCAAAGGCAGGT	57.3	199
PIN16 RT-R4	Reverse	GGATAGTTTCAACATGGTCCCTCTCA	58.2	
AUX1 RT-F1	Forward	TCCCTTTATGCCAAGCTGGA	56.5	217
AUX1 RT-R1	Reverse	ATGTAGTCAGCTCACTCAGCG	56.6	
AUX2 RT-F3	Forward	CGTTCGGACTCTTCGCAAAG	56.3	100
AUX2 RT-R3	Reverse	TCTTGGGACTGATTTGCTTCAG	55.1	
AUX3 RT-F2	Forward	GTTCACGGCCAGGTTGATG	56.6	100
AUX3 RT-R2	Reverse	CATGCCCACCAAAAGTGTAGAG	56.1	
AUX4 RT-F4	Forward	AGGGTGGGCTAGTATGTCCAA	57.7	191
AUX4 RT-R4	Reverse	AAACACAATGCAGAGGAGATGC	55.9	
AUX5 RT-F1	Forward	AGCCATCAAAGTACACGGGA	56.3	174
AUX5 RT-R1	Reverse	TCTGAGGTGGGCATTGGTAA	56.1	
AUX6 RT-F4	Forward	CCTGTGGTTATTCCCATTTGGTT	55.6	180
AUX6 RT-R4	Reverse	GTACTTTGGTGGTTGCTCCA	55.2	
AUX7 RT-F2	Forward	CGTCAGATTGATTCATTTGGTCTATTC	54.2	213
AUX7 RT-R2	Reverse	ATCACACCTTTTCAAGAACCAACA	55.2	
AUX8 RT-F1	Forward	GAGAGAATGCTGTGGAGAGAC	54.8	182
AUX8 RT-R1	Reverse	ACACTGGTAGCACTTGGTGA	56.2	
ABCB1 RT-F4	Forward	GATGGTAAAGTAGCAGAGCAAGGAT	56.7	212
ABCB1 RT-R4	Reverse	ATGGGATATACTCCTCTTACTGGTGT	56.5	
ABCB2 RT-F3	Forward	CAAGCATGAGACTCTGATTCATATCA	54.7	100

(Continued)

Table A5 | Continued

Name	Direction	Sequence (5′–3′)	Tm (°C)[a]	Amplicon (bp)
ABCB2 RT-R3	Reverse	AATATTGCAGGTGGTGACTCAAGA	56.4	
ABCB4 RT-F2	Forward	GGGCAATCCTAAAGAATCCGAAAAT	55.7	264
ABCB4 RT-R4	Reverse	TATGAAGGGCGACCAAGGATG	56.9	
ABCB5 RT-F3	Forward	TCGCAATACCTCCCGGTACA	58.1	100
ABCB5 RT-R3	Reverse	GCGTGCGGGTCGTAAAAC	57.3	
ABCB7 RT-F2	Forward	GTGGTTTTGCTGTTAGATGAGGC	56.5	269
ABCB7 RT-R2	Reverse	ACTGTTTTGTGTTGTCCTCTGG	55.4	
ABCB10 RT-F4	Forward	CAG AAG CAA AGG GTA GCC ATT	55.4	211
ABCB10 RT-R4	Reverse	CTCCATTTTTAACCACTGCGATTAGA	56.4	
ABCB13 RT-F3	Forward	CAAGAGCAATTCTGAAAGATCCACG	56.3	206
ABCB13 RT-R3	Reverse	ACCTTTTTCCACTATCTTGCCATG	55.6	
ABCB14 RT-F1	Forward	GACAGTCAAGTCAAAGAATCTCATTG	54.2	221
ABCB14 RT-R1	Reverse	TGGAACCTCTGGCTTGTTAAGA	56	
ABCB13 RT-F2	Forward	CAAGAAGCACTGGACCGAATCAT	57.4	229
ABCB13 RT-R2	Reverse	TAAACACACGGAGGTGCTACAAT	56.4	
ABCB18 RT-F3	Forward	AGCTCATCCATCGAATCTGAATCAA	56.3	211
ABCB18 RT-R3	Reverse	GCATCAGACGGACATACAAACCAT	57.4	
ABCB19 RT-F3	Forward	TCTTAAGGACCCAGCAATCCTACT	57.3	100
ABCB19 RT-R3	Reverse	CCTCATTAGCCTCTCGAGTGCTT	58.5	
ACT2 RT-F1[b]	Forward	GCAACTGGGATGATATGGAGA	54.3	213
ACT2 RT-R1	Reverse	TACGACCACTGGCATACAGG	56.5	
UBQ RT-F1[b]	Forward	CAGCTTGAAGATGGGAGGAC	55.4	154
UBQ RT-R1	Reverse	CAATGGTGTCTGAGCTCTCG	55.5	
TUA2 RT-F1	Forward	CCTACTGTAGTACCTGGGGGTG	58.2	230
TUA2 RT-R1	Reverse	CCAACTTCCTCGTAATCCTTCTCA	56.2	
PD-E1 RT-F1	Forward	ATGAGAACTGGTGGTATTGGTGC	57.3	164
PD-E1 RT-R1	Reverse	GTCACAATCTGGGCAGGTTGAAC	58.5	
CLONING AND SEQUENCING				
M13F	Forward	TTGTAAAACGACGGCCAGT	54.7	
M13R	Reverse	CAGGAAACAGCTATGACC	50.1	
adp1-dT17[c]		CCGGATCCTCTAGAGCGGCCGC(T)$_{17}$	64.6	
adp1		CCGGATCCTCTAGAGCGGCC	61.9	
PIN3 RT-F3	Forward	CTTCACGTTGCTATTGTTCAGG	54.1	
PIN4 RT-F3	Forward	CTTCAGCCTCGGATAATTGTATGC	55.1	
PIN11A RT-F3	Forward	GCGATGTCTTACGTGTTGCTA	55.1	
PIN13 RT-F2	Forward	GGATACATTGAGCACAGGGGTAA	56.6	
AUX4 RT-F3	Forward	CCGACTCCTGCAAAACATCATTA	55.4	
ABCB1 RT-F3	forward	CGCATGATACAGTTACAAAGGTTCA	55.5	

[a]*Melting temperatures were calculated with the online tool OlygoAnalyzer v.3.1 from Integrated DNA Technologies.*

[b]*These primer pairs have been first published in Secchi et al. (2009).*

[c]*This primer sequence has been first published in Kramer et al. (1998).*